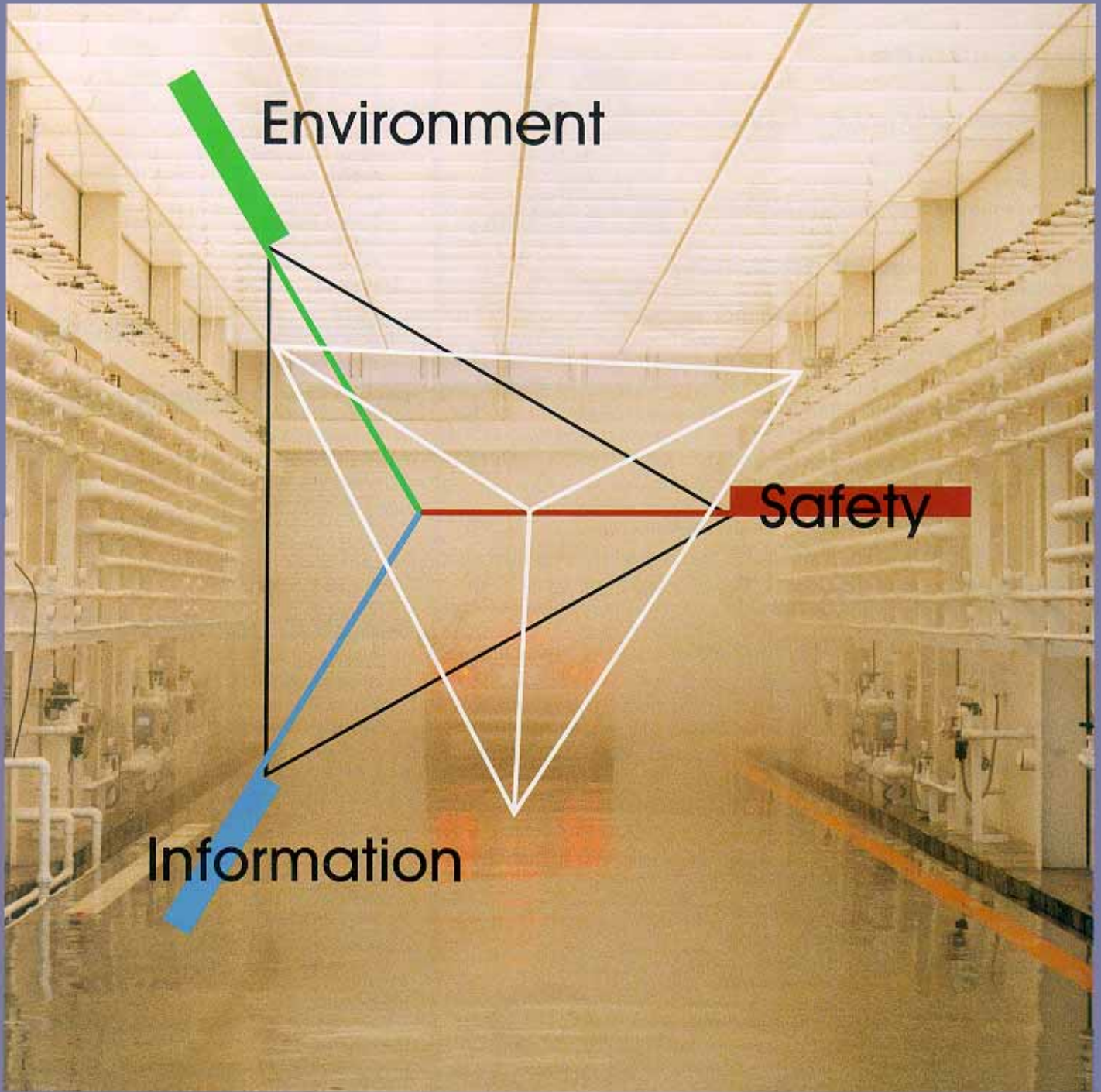


VOL. 78/MAR. 1997

MITSUBISHI ELECTRIC

ADVANCE

Automotive Electronics Edition



Automotive Electronics Edition

CONTENTS

TECHNICAL REPORTS

FOREWORD

To the Special Edition on Automotive Electronics 1
by Masanobu Tosa

OVERVIEW

The Present and Future Trends in Automotive Electronics 2
by Dr. Shoichi Washino

A Car Navigation System with Traffic Information Capabilities 4
by Yoshisada Mizutani and Toshiro Sogawa

A Digital Audio Broadcast Receiver 7
by Hiroaki Kato and Ken'ichi Taura

Vehicle Distance Interval Control Technology 10
by Kazumichi Tsutsumi and Shigekazu Okamura

A Drowsiness Detection System 13
by Kenji Ogawa and Mitsuo Shimotani

Motor-Drive Control Technology for Electric Vehicles 17
by Kazutoshi Kaneyuki and Dr. Masato Koyama

An Electric Power-Steering System 20
by Takayuki Kifuku and Shun'ichi Wada

Technologies for Gasoline Engine Control and ECU Miniaturization 24
by Yoshinobu Morimoto and Takanori Fujimoto

Starting and Charging Systems for Fuel-Efficient Engines 28
by Toshinori Tanaka and Akira Morishita

NEW PRODUCTS 31

MITSUBISHI ELECTRIC OVERSEAS NETWORK

The background photograph for our cover was taken at our laboratory simulating natural environments. This is used to assess safety factors. Fifty meters long, it can simulate dense fog, torrential rain, and intense lighting under strictly controlled conditions

Editor-in-Chief

Akira Yamamoto

Editorial Advisors

Jozo Nagata
Toshimasa Uji
Tsuyoshi Uesugi
Satoru Isoda
Masao Hataya
Gunshiro Suzuki
Hiroshi Shimomura
Hiroaki Kawachi
Akihiko Naito
Nobuo Yamamoto
Shingo Maeda
Toshikazu Saita
Hiroshi Tottori
Masaaki Udagawa

Vol. 78 Feature Articles Editor

Yukiyasu Watanabe

Editorial Inquiries

Masaaki Udagawa
Planning and Administration Dept.
Corporate Engineering, Manufacturing &
Information Systems
Mitsubishi Electric Corporation
2-3-3 Marunouchi
Chiyoda-ku, Tokyo 100, Japan
Fax 03-3218-2465

Product Inquiries

Tsuyoshi Uesugi
Strategic Marketing Dept.
Global Operations Group
Mitsubishi Electric Corporation
2-2-3 Marunouchi
Chiyoda-ku, Tokyo 100, Japan
Fax 03-3218-3597

Orders:

Four issues: ¥6,000
(postage and tax not included)
Ohm-sha Co., Ltd.
1 Kanda Nishiki-cho 3-chome
Chiyoda-ku, Tokyo 101, Japan

Mitsubishi Electric Advance is published quarterly (in March, June, September, and December) by Mitsubishi Electric Corporation. Copyright © 1997 by Mitsubishi Electric Corporation; all rights reserved. Printed in Japan.

Foreword

to the Special Edition on Automotive Electronics

*Masanobu Tosa**



Advances in electronics and communications technologies are responsible for making our society increasingly information oriented. Now that cars are being fitted with portable telephones and other equipment for inter and intra-car communications, they are no longer largely isolated from these trends and are becoming ever more closely integrated with society, sharing in its information and communications infrastructure. This is typified by research into intelligent transport systems (ITSs). Mitsubishi Electric is engaged in a wide range of ITS research and development projects, including semiconductor devices, in-car equipment, millimeter-band and optical communications equipment, and the technologies for system operation.

ITS-related equipment includes navigation systems, which are now coming into widespread use. Other important topics include the development and implementation of technologies for automating the actual processes of driving a car and improving safety. The corporation's research and development for navigation systems is aimed at enhanced functionality, including making them suitable for all geographical areas of the different countries, improved man-machine interfaces, etc. Again, in automatic driving and safety technology, we are committed to R&D for the sensors and control techniques that are essential for reliable systems that optimize the car's basic performance capabilities.

In a society that is so heavily dependent on the car, we cannot ignore environmental concerns. Here, we can make a contribution not only by manufacturing in-car equipment in factories that are operated responsibly but also by making it smaller and lighter, and by optimizing the various control functions. □

**Managing Director Masanobu Tosa is in charge of the Automotive Equipment Group.*

The Present and Future Trends in Automotive Electronics

by Dr. Shoichi Washino*

Over the three decades from the 1960s to the 1990s, the motor vehicle industry has gradually introduced electronic technology to perform many of the control functions previously performed mechanically. This report surveys developments in electronics technology and their practical applications.

Background

Three factors have stimulated motor vehicle manufacturers to adopt electronic control in a increasing number of motor vehicle systems: advances in semiconductor technology, more stringent environmental regulations, and user demand for enhanced performance and convenience. In addition, the popularity of car navigation systems reflects the growing demand for information technology in the automotive environment.

Table 1 shows a chronology of advances in automotive electronics in the context of related technologies. Breakerless electronic ignitions were first introduced in the 1960s and soon proved their reliability. Gradually electronic components began to replace other mechanical components. The 1970s saw the introduction

of electronic fuel-injection systems and marked the beginning of a rapid changeover from mechanical to electronic control technologies. Electronic fuel injection showed that not only could electronic components substitute for mechanical components but that electronic control systems could radically alter the way that motor vehicles perform.

In the 1980s, electronic fuel-injection systems were supplemented by additional electronics for controlling ignition timing and exhaust gas recirculation (EGR) systems. Electronic control systems began to take on a comprehensive character reflected in a new term: engine control systems. Manufacturers also started using electronics for ABS and other chassis control applications. The 1990s have brought car phones, navigation systems and other information equipment into the automotive environment.

Technological Advances in Electronic Systems

FINE-PATTERN LITHOGRAPHY. Improvements in semiconductor processing technologies bring a quadrupling of device integration scale approxi-

Table 1 Chronology of Automotive Electronics Technology.

	1960	1970	1980	1990	2000			
Events affecting Japan		Expo '70 in Osaka	First and second oil crises Automotive exhaust gas regulations	Bubble economy	High yen Diesel exhaust gas regulations			
Technology Trends	Hardware	DRAM Microprocessors	4-bit 8-bit	256kB 16-bit	1Mb 32-bit	16Mb 64-bit	64Mb	1Gb
	Software	Languages	Fortran, Cobol	PL/1	Pascal, ADA, C			
		Personal computer operating systems		CP/M	MS-DOS	Windows 3.1	Windows 95	
Communications	Phones for electrical trains	First data transmission services and digital telecommunications		Car phones, Fax machines,	Cellular phones, Packet transmission	PHS	Compact satellite terminals	
Automotive electronics	Information				Vehicle information and communication systems for navigation			
	Chassis			ABS	Suspension, Power steering	4WD, 4WS	Distance interval control systems	
	Engine	Electronic ignition		Electronically controlled AT, Electronic fuel injection		Electronic combustion control, Electronic valve timing control, Per-cylinder knock control		
	Body	Intermittent wipers		Automatic air-conditioning control Drive computer			Keyless entry	
	1960	1970	1980	1990	2000			

*Dr. Shoichi Washino is with the Industrial Electronics & Systems Laboratory.

mately every three years in a growth curve referred to as Moore's Law. Today, 64Mb DRAM devices are commercially available, and laboratories are already manufacturing samples of 1Gb DRAMs. In practical terms, this higher integration gives manufacturers the ability to offer sophisticated control capabilities at a low cost through use of application-specific integrated circuits (ASICs) and micromachined semiconductor sensors. We can anticipate that manufacturers will soon introduce system-on-chip (SOC) devices combining microprocessors, memory, software and peripheral circuitry in a single device.

MICROSYSTEM TECHNOLOGIES. Microsystems incorporate sensors, microactuators and microprocessors on a single chip, allowing entire control functions to be implemented in a single device. Micromachining technology has already given us semiconductor acceleration and pressure sensors. Improvements in sensor accuracy and reductions in size and cost will follow as micromachining and surface processing technologies continue to evolve. The near future is expected to bring intelligent sensor devices integrating microprocessors, memory, ASIC technology and sensor elements on a single chip.

MATERIALS AND DISPLAY TECHNOLOGY. Advances in materials and processing technologies promise to bring about significant developments in monolithic microwave ICs (MMICs), room-temperature infrared sensors, blue-wavelength semiconductor lasers and optical amplifiers. Advances are also expected in the liquid-crystal and plasma panels used to display information in car navigation systems and other applications.

STANDARDIZED SOFTWARE. Faster microprocessors and cheaper memory are giving embedded system designers latitude to build more sophisticated systems. The high development costs of these systems remain as a significant obstacle. Future applications will most likely require a combination of standardized and customized software to realize complex systems with the reliability required of motor vehicle

control systems at an acceptable cost.

NETWORKING TECHNOLOGY. Active work on automotive LAN standards is underway, with standards for three automotive LAN systems (Class A, B and C) currently under development. We can expect that future vehicles will also be linked to wide-area networks such as the Internet through cellular phones, leased lines or other means. The tremendous popularity and utility of the global positioning system (GPS) suggests a promising future for other satellite-based applications.

Comprehensive Control Systems

INTEGRATED TRAVEL CONTROL SYSTEMS. We can envisage a comprehensive travel control system integrating vehicle ECUs and travel monitoring sensors over an automotive LAN. Such systems could be enhanced by sensors monitoring roadway conditions and the distance interval between vehicles.

INTELLIGENT TRANSPORT SYSTEMS. In November 1995, participants from Japan, Europe, North America and other nations met in Yokohama, Japan, to discuss the future of intelligent transport systems (ITS) and other means to facilitate safe, smooth transportation using intelligent communication between vehicles and the roadway. We can anticipate that the roadway infrastructure will eventually be enhanced with telecommunication capabilities and corresponding equipment will be developed for motor vehicles.

Mitsubishi Electric is conducting R&D on all the key hardware, software and networking technologies presented in this report. The corporation is committed to the development of automotive electronics for applications ranging from stand-alone components to comprehensive control systems as well as new-generation systems with telecommunication capabilities. □

A Car Navigation System with Traffic Information Capabilities

by Yoshisada Mizutani and Toshio Sogawa*

Mitsubishi Electric has developed a car navigation system capable of displaying traffic information from Japan's Vehicle Information and Communication System (VICS). This article reports on functions that overlay roadway maps with symbols showing traffic jams and other data, and driver-guidance functions using sketch maps and synthesized voice announcements.

Car Navigation Using VICS

Japan's Vehicle Information and Communication System (VICS), in operation since April 1996, transmits realtime information on traffic jams, accidents, roadway obstructions and other pertinent phenomena to vehicles using a combination of FM multiplex broadcasts, radio beacons and infrared beacons (Fig. 1, Table 1). The car navigation system we developed superimposes this information on the main map display. The information is also available for indicating traffic jams and other obstructions on sketch maps of the planned route, and for searching for alternative routes.

VICS provides three levels of information intended for car navigation systems of varying types. Level 1 consists exclusively of text information. Level 2 consists of simplified maps showing traffic jams and obstructions.

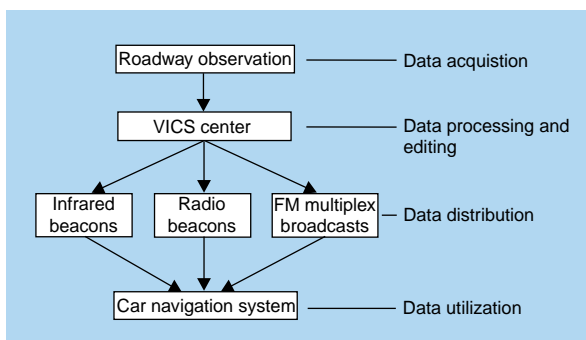


Fig. 1 The VICS system. The arrows show the direction of information flows.

Table 1 Media Used to Distribute VICS Information

Medium	Data rate	Remarks
FM multiplex broadcast	Approx. 50KB/5 minutes per station	Wide-area data distribution to all vehicles in broadcast service area
Radio beacons	Approx. 8KB per beacon	Installed along freeways to inform drivers of conditions ahead
Infrared beacons	Approx. 10KB per beacon	Installed above roadways to inform drivers of conditions ahead

Level 3 provides detailed maps and includes four types of information. Traffic jam data shows the precise location of jams and the corresponding transit delays. Accident data describe accidents and other phenomena that obstruct traffic, and indicate the severity of the obstruction. Parking information shows the locations and names of roadway service areas and parking areas, and their degree of crowding. Travel time data reports the transit times between specific points.

Superimposed Display

Drivers can manually request the display of level 1 and level 2 data. Level 3 data includes a numerical code indicating the roadway to which it applies. This allows the car navigation system to selectively display information relevant to the vehicle's planned or actual route.

Figs. 2 and 3 show how these data are included in the map display. In Fig. 2, traffic jam, roadway obstructions and parking data are shown visually. Traffic jams are shown by a chain of arrowheads that indicate the length of the jam and the direction of traffic affected. The arrows are shifted slightly to the left to avoid interfering with the lines that indicate the roadway and recommended route. The arrows always appear beneath the recommended route for better legibility.

Fig. 3 shows a map display with a text window for detailed accident and roadway obstruction data. The driver can also call up detailed parking availability data. The side-by-side format is easy to read and does not interfere with normal use of the navigation system.

Guidance by Sketch Map and Voice

Most car navigation systems provide route guidance using a combination of enlarged intersection drawings and synthesized voices. The draw-

*Yoshisada Mizutani and Toshio Sogawa are with the Sanda Works.

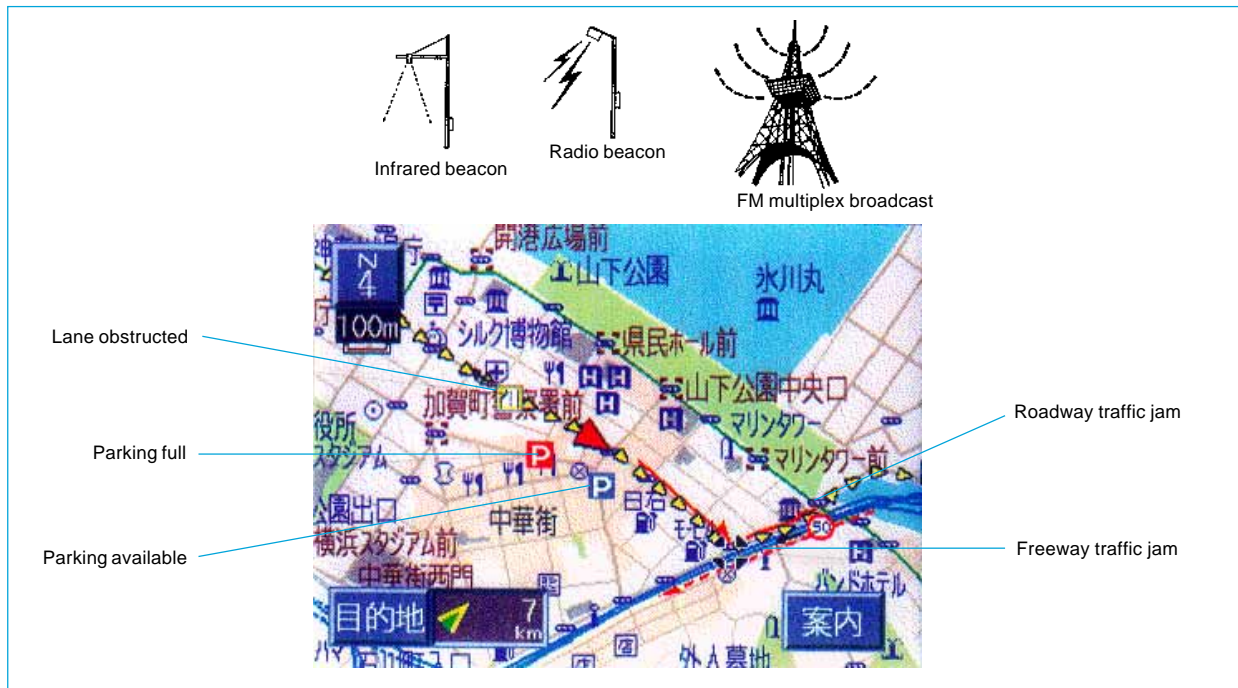


Fig. 2 Traffic information superimposed on a map display.

ings indicate the path of travel, the distance to the next turn and nearby landmarks (Fig. 4). Since

the demands of driving permit drivers to view the navigation screen only briefly, simplified displays are needed so that drivers can assimilate information rapidly and without strain. This led us to investigate drivers' mental representations of roadway networks—which we refer to as cognitive maps—and to design the user interface to present information in a manner that is consistent with these representations.



Fig. 3 Detailed information on obstructed lanes.

Cognitive maps are characterized by quantization of direction and distance between significant points, representation of links between points by straight lines and the mental conversion of graphic images to propositional images. Figs. 5 and 6 show the simplified sketch maps we developed for route guidance. Fig. 5 shows a map of an intersection where a turn is required, and Fig. 6 an overview of the planned route. In both cases only essential information is provided. The direction and distance information between points is quantized, and the path between points is represented by straight lines.



Fig. 4 Detailed drawing of a guidance point.

The intersection maps usually show roadway angles in increments of 45 degrees. A 30-degree quantization is used for more complicated intersections where 45-degree quantization would cause roadways to overlap. Intersections where the roadways are at a slight angle are represented using right angles. This simplification is consistent with drivers' cognitive mapping and improves map recognition.

The sketch maps are always oriented north up. Intersections are joined by straight lines using quantized distances and the roadway



Fig. 5 Sketch map of a guidance point.



Fig. 6 Sketch map of a planned route.

Table 2 Information Content of Sketch Maps and Synthesized Voice Guidance

Time	Screen	Voice
About 1km before turn	No display	1. Location specifier: transit, destination, ferry port, freeway on-ramp, freeway off-ramp Example: 'Nearing transit point. Take freeway off-ramp'
		2. Direction Example: 'Left turn'
		3. Distance Example: '1km ahead'
Immediately before turn	1. Location specifiers: intersection shape, intersection name, landmarks	1. Location specifier: transit, destination, ferry port, freeway on-ramp, freeway off-ramp Example: 'Nearing transit point. Take freeway off-ramp'
	2. Route identifier	
	3. Vehicle position indicator	2. Direction Example: 'Left turn'
	4. Numerical distance-to-turn display	

angles near the intersections are maintained.

Table 2 shows how the task of conveying information to the driver is distributed between the screen and synthesized voice output. The system first provides the driver with advanced notice of an upcoming turn. A synthesized voice announces the distance to the turn and the direction the driver will be required to turn. This reduces the mental workload by enabling the driver to prepare for the action. As the driver approaches the turn, the screen displays a sketch map of the intersection and the synthesized voice advises the driver of the direction to turn.

The driver can also set up the system so that information requests are answered by both synthesized voice and screen display.

Through skillful integration of roadmaps, superimposed traffic information, simplified maps at turns on the planned route and synthesized voice announcements, this car navigation system provides drivers with information in easily assimilated form with a minimal mental workload. Further development is planned to enhance these benefits for improved driving safety and convenience. □

A Digital Audio Broadcast Receiver

by Hiroaki Kato and Ken'ichi Taura*

FM broadcasts are subject to multipath interference that causes impairment of sound quality when the signal is received by a moving vehicle. To solve this problem and provide audio broadcasting of compact disk quality, the European Eureka project developed a digital audio broadcasting (DAB) system. DAB public services have been operational and on air in the UK since September 1995, and are expected to spread widely throughout Europe by fall 1997.

The DAB System

The DAB system uses ISO/MPEG1 audio coding for source coding and orthogonal frequency division multiplexing (OFDM) for modulation.

MPEG1 is a highly efficient source coding technique. It allows bit rate reduction by utilizing a psychoacoustic model of the human ear, thus preserving the subjective quality of the audio signal. The audio frequency range is divided into 32 sub-bands of equal width. Every sub-band is allocated a bit capacity based on the difference between the maximum signal level and audible threshold, which is calculated from the threshold of audibility at silence and the masking threshold.

OFDM is a multicarrier scheme which transfers high-speed data using a number of orthogonal carriers with tight frequency spacings. When combined with error correction code, it is called coded OFDM (COFDM). Each carrier is modulated by $\pi/4$ differential quadrature phase shift keying (DQPSK). Even if some of the carriers are degraded by frequency-selective fading due to multipath propagation, the data of these carriers can be recovered from the data of the remaining carriers by performing error correction.

Fig. 1 shows the transmission frame format of the DAB system. Each frame consists of multiple symbols. The first frame is a null symbol which is the duration of no radio frequency (RF) signal transmission, and is used for frame synchronization. The second frame is a phase reference symbol for QSPK demodulation, which is followed by two symbol groups. One is a fast information channel (FIC), and the other is a main service channel (MSC). The FIC transmits program related information and the multi-

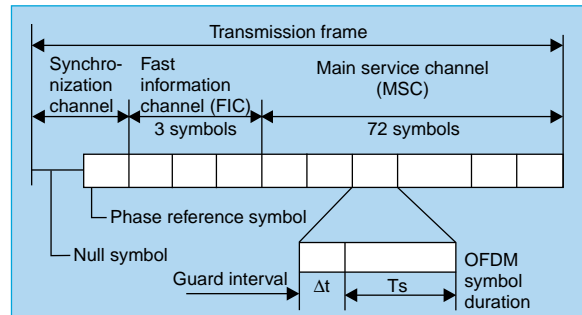


Fig. 1 Transmission frame.

plex configuration information of the MSC. The MSC transmits audio programs and various data service information.

Each symbol consists of a useful symbol duration (T_s) and a guard interval (Δt), in which, part of the time, a signal of T_s is cyclically repeated. As long as the multipath propagation delays do not exceed the duration of the interval, no inter-symbol interference occurs and no channel equalization is required. This enables a broadcast network to be extended virtually without limitations by operating all transmitters on the same radio frequency; known as a single-frequency network (SFN).

Table 1 lists four transmission modes available in the DAB format, each of which supports a bandwidth up to 3GHz.

Table 1 General DAB Specifications

	Mode I	Mode II	Mode III	Mode IV
No. of radiated carriers	1,536	384	192	768
Frame duration	96ms	24ms	24ms	48ms
Null symbol duration	1,297 μ s	324 μ s	168 μ s	648 μ s
Useful symbol duration	1,000 μ s	250 μ s	125 μ s	500 μ s
Guard interval	246 μ s	62 μ s	31 μ s	124 μ s
Nominal freq. range (for mobile reception)	375MHz	1.5GHz	3GHz	1.5GHz
Suitable communication applications	Single-freq. terrestrial networks	Terrestrial/satellite communications	Satellite communications	Terrestrial communications

*Hiroaki Kato is with the Sanda Works and Ken'ichi Taura with the Imaging Systems Laboratory.

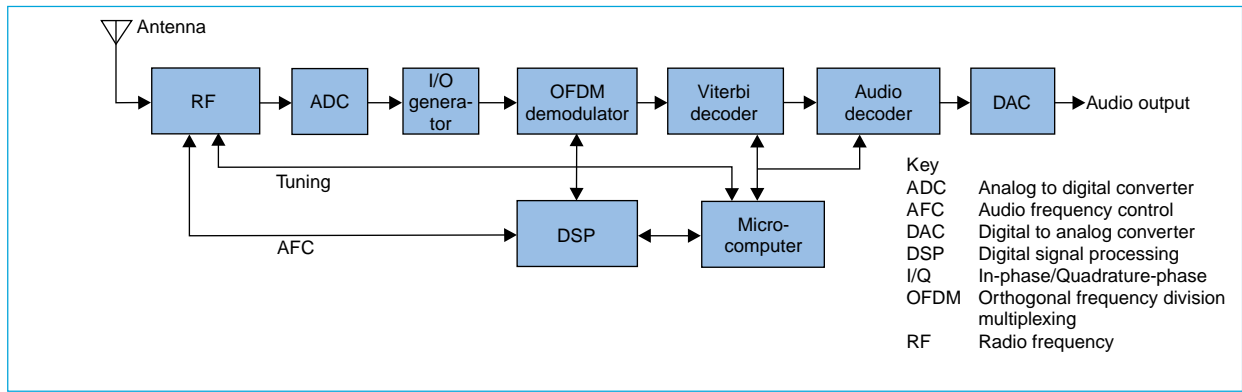


Fig. 2 Block diagram of a DAB receiver.

A DAB Receiver

Fig. 2 shows a block diagram of a DAB receiver developed by Mitsubishi Electric. The RF block can receive both VHF and L-band signals, and converts them to intermediate frequency (IF) signals. The IF signals are converted to digital signals by an A/D converter (ADC). The digital signals are then converted to in-phase and quadrature components and fed into the OFDM demodulator. Here, the orthogonal carriers are derived from the time signal on a symbol basis by means of a fast Fourier transform (FFT) processor. After this, the data is reproduced by a DQPSK modulator from each carrier. A Viterbi decoder executes the time and frequency interleaving and error correction for the reproduced data. An MPEG1 audio decoder expands the coded audio data to linear PCM audio data, which is then converted to analog audio signals by a D/A converter (DAC). A 16b general-purpose digital signal processor (DSP) is utilized for the synchronization process of the received signal to fulfill the requirement of frequency and timing accuracy.

FFT is executed on a useful symbol duration. Each carrier has a peak position where all others have zero-crossings if a carrier-spacing equals $1/T_s (=f_0)$. This orthogonal relationship prevents inter-carrier interference.

Frequency offset of a local oscillator of a RF block disturbs the orthogonal relationship. This causes degradation of the carrier-to-noise (c/n) ratio due to inter-carrier interference, and results in degradation of the error rate. We measured the bit error rate in relation to the frequency offset of local oscillators. In the case of Mode I transmissions, the bit error rate is degraded markedly at an offset larger than 50Hz. Considering this, our objective was a frequency synchronization accuracy of 25Hz, which corresponds to 0.1ppm precision in a 220MHz signal.

Frequency synchronization is generally controlled as follows. The local oscillator is adjusted

to the frequency at which the phase difference between the phase of received data after demodulation and the possible phase point of reproduced data by the receiver during synchronization becomes zero. However, if the phase difference due to frequency offset exceeds $\pi/4$, an alias-lock on the frequency with errors corresponding to a multiple of $\pm\pi/2$ may occur. We therefore investigated control methods utilizing information related to received signal level and phase of each carrier, which is obtained by FFT execution on the received signal.

As shown in Fig. 3, when a direct wave and reflective waves due to multipath propagation are received, intersymbol interference will occur in the signals received by the RF block. In the DAB system a guard interval is inserted between successive symbols, enabling the reproduction of signals free from multipath propagation by executing FFT for the duration of no intersymbol interference.

In DQPSK modulation, data is transmitted by the relative phase difference between adjacent symbols. Therefore, FFT must be executed in the same position of each symbol duration.

These requirements can be fulfilled by executing FFT from the end point of the guard intervals of the direct wave. We investigated calculating the reference point of the direct wave within the symbol duration from the impulse

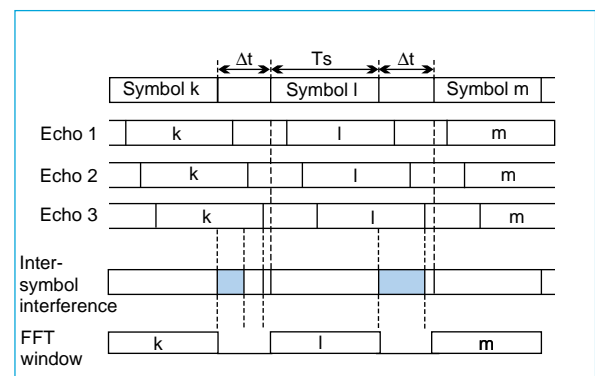
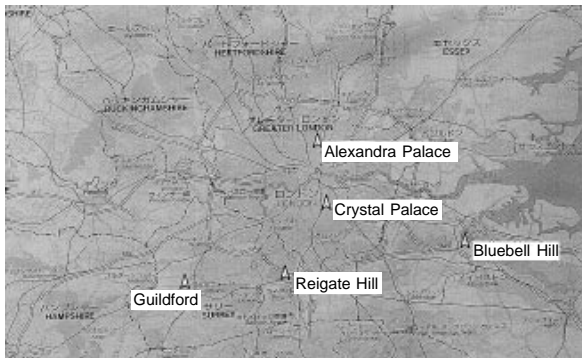


Fig. 3 Constructive contribution of echoes.

response of the transmission channel.

Field Tests

We carried out field tests in the UK (London)



Name	Location	Approx. power
Crystal Palace	South Central London	4kW ERP
Bluebell Hill	East of London	1kW
Alexandra Palace	North London	1kW
Reigate Hill	South London	1kW
Guildford	Surrey (South)	1kW

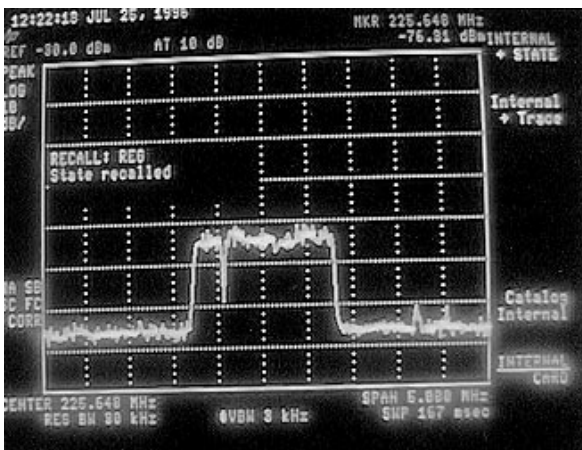
Fig. 4 Transmitters in the BBC's DAB network in London.

for the purpose of verifying the reception performance of the newly developed DAB receiver and FIC data collection. Fig. 4 shows BBC transmitter locations and the radiation power in London and its suburbs. In the moving vehicle test around Surrey Research Park in Guildford, interference-free sound reception was confirmed under the electric field conditions of Fig. 5a. We also confirmed interference-free reception under a multipath environment. In such environments, reception of the same programs using other FM broadcast receivers suffered from multipath noise. We could therefore confirm the superiority of the DAB system.

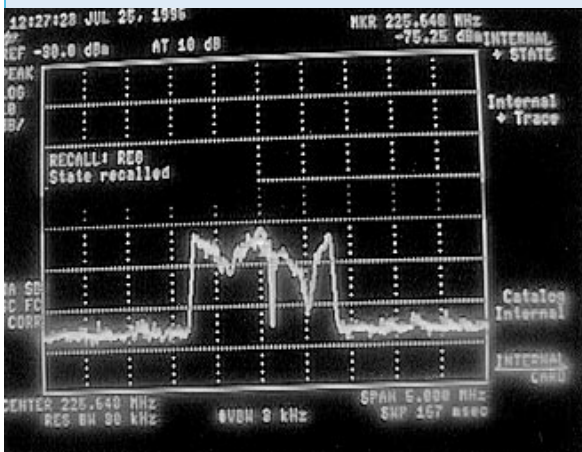
We also conducted a reception test at Dorking, midway between the Reigate and Guildford transmitters, to test reception at the fringe of the SFN transmitter service area, where field strength becomes poor due to interference caused by each transmitter's signal (Fig. 5b). The field strength was -80dBm , -90dBm when picked up on a receiver in a moving vehicle at high speed. Under such conditions, the receiver could reproduce an audio program without audible noise. Through these tests, we confirmed that a mobile DAB receiver requires a sensitivity of -96dBm to cover the SFN service area thoroughly.

During the above tests, the following FIC data were collected; MSC configuration data, label and language information, date and time information (including local offset), reconfiguration data of service and subchannel organization.

We have developed a prototype DAB receiver and confirmed the superiority of DAB systems through field tests and subsequent mobile reception tests. Considering the results of these tests, utilizing BBC regular services, we hope to develop a widely acceptable commercial DAB receiver with superior reception sensitivity and a variety of functions. □



a) Spectrum waveform at Guildford



b) Spectrum waveform at Dorking

Fig. 5 Spectrum waveform measurements.

Vehicle Distance Interval Control Technology

by Kazumichi Tsutsumi and Shigekazu Okamura*

Technical advances can make the task of driving a vehicle safer and more pleasant. This report introduces a distance interval control system for vehicles that supplements the capabilities of conventional cruise control. The system uses a laser radar system to identify preceding vehicles, processes images from a CCD camera to identify one's own lane of travel, finds the closest vehicle in the lane and then controls the throttle to establish a safe following distance. The system combines two thoroughly understood technologies: active laser radar and passive image processing.

Configuration

The system, illustrated in Fig. 1, consists of a laser radar system, a CCD camera, sensors for speed, steering wheel angle and other automotive parameters, a throttle actuator, an electronically controlled automatic transmission, an alarm buzzer and a controller.

Laser Radar Head

Fig. 2 shows the laser radar head's scanning mechanism. On receiving a signal from the controller, a motor-driven cam scans a mirror back and forth under microprocessor control. Light emitted by the laser diode is directed by a fixed mirror to the scanning mirror and projected forward from the car creating a fan-shaped beam. Reflectors on vehicles and other objects return the beam through the receiving lens to a photodiode. The microprocessor measures the time required for the reflection to return and uses that information to compute the distance information, which it sends to the controller.

A dirty front windshield, rain, snow or water kicked up by the preceding vehicle can all degrade the performance of a laser radar system. We studied these effects in a roadway environment simulation facility (Fig. 2) and installed a sensor near the laser diode that detects a dirty windshield and reports this to the microprocessor.

Preceding Vehicle Detection Algorithm

A single scan by the laser radar system collects distance data in 80 directions. Reflectors on cars

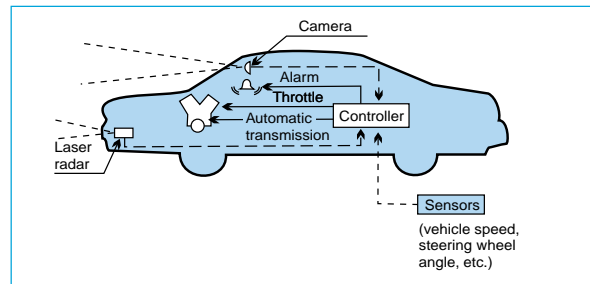


Fig. 1 The system configuration.

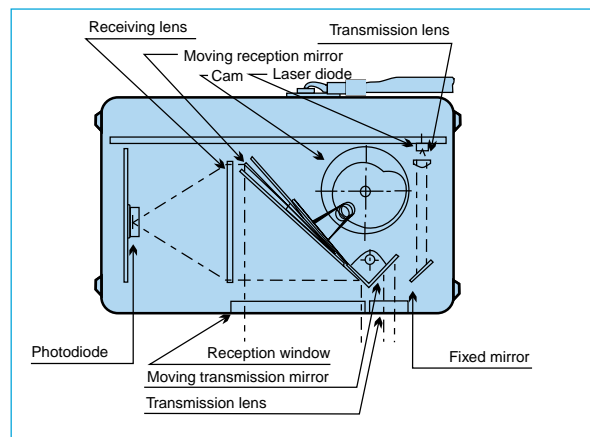


Fig. 2 Laser radar optics.



Fig. 3 Natural environment simulation facility.

and trucks or along the roadside result in numerous adjoining data points. Several steps are required to resolve this data into individual reflectors and then to identify vehicles. Fig. 4 illustrates this process.

The solid boxes in the figure show where measurement points have been grouped to iden-

*Kazumichi Tsutsumi and Shigekazu Okamura are with the Himeji Works.

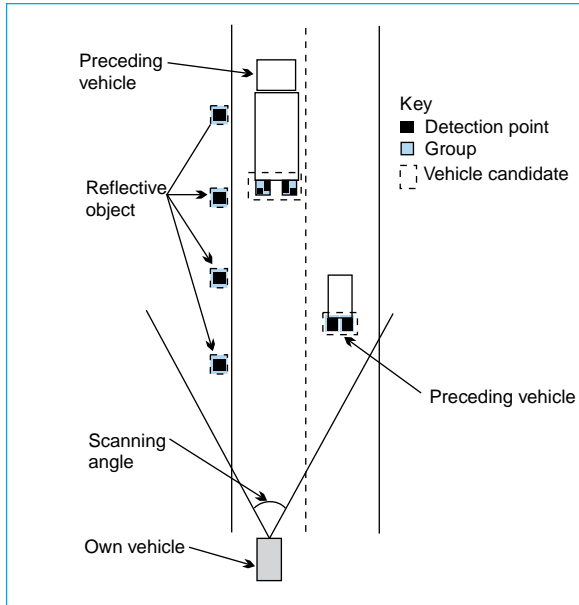


Fig. 4 The vehicle detection algorithm.

tify individual reflectors. Next, position and movement data are used to associate reflectors into larger groups that correspond to vehicles or other objects. Steering displacement data is then used to identify other vehicles traveling in the same direction.

The next stage of processing uses lane information extracted by processing an image from the CCD camera. Vehicles in the lane of travel are identified, and the distance to the nearest is returned as the vehicle distance interval.

Lane Detection Algorithm

The image processing system analyzes CCD camera images of the roadway to identify painted lane markers. These lines may be soiled, worn away or completely absent. The system deals with these possibilities by first identifying edges in the image, and then examining the edges to identify lines marking the lane of travel. The detection algorithm identifies the lane of travel by searching for boundaries that are stable with respect to time for vehicle speeds over a certain threshold. The lane width is used as auxiliary criteria, since lane widths tend to fall within a particular range.

Once the left and right lane edges are found,

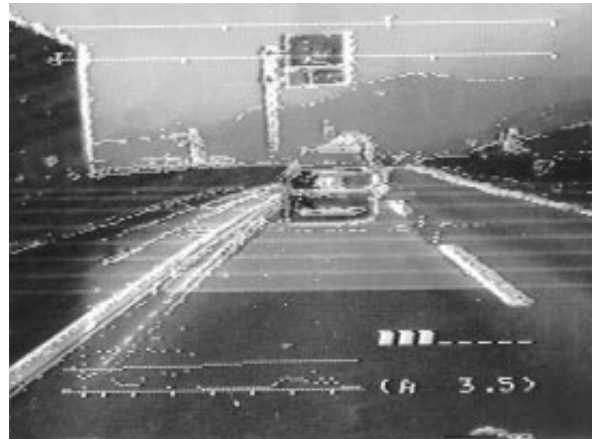


Fig. 5 Lane detection.

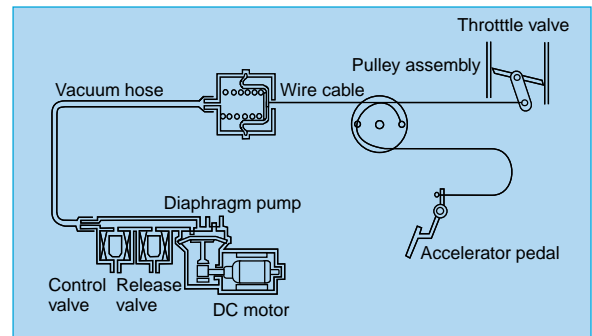


Fig. 6 Accelerator actuator.

the region in between them is known, making it possible to determine if a particular vehicle is in one's own lane of travel. Fig. 5 shows a processed image used for lane marker detection.

Actuators

The throttle actuator, shown in Fig. 6, consists of an electric-motor-driven diaphragm vacuum pump, two solenoid valves and a vacuum-driven throttle actuator. The vacuum generated by the diaphragm pump is supplied to the actuator's vacuum chamber. The electric motor and the switching of the two solenoid valves control the throttle position.

Vehicle Distance Interval Control

This section describes several operational scenarios.

If no preceding car is detected, vehicle speed is determined by the cruise control, which

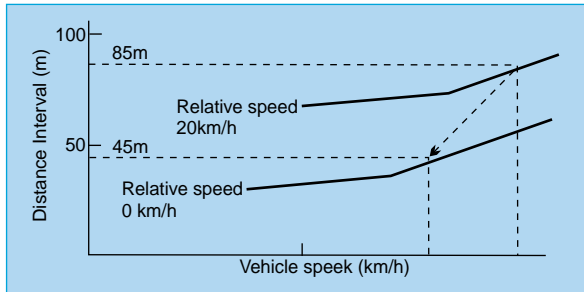


Fig. 7 Initial control.

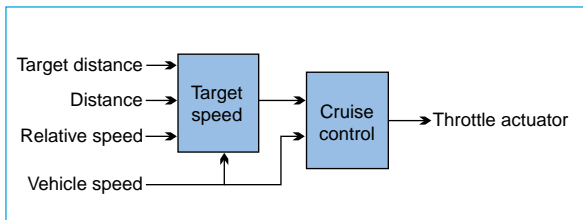


Fig. 8 Vehicle speed control logic.

maintains the vehicle at a driver-selected speed.

As the car approaches another vehicle, the vehicle speed is used to determine an appropriate following distance, and the throttle and transmission are adjusted to establish and maintain this distance. Initial control parameters are based on the vehicle speed and relative speeds of the two vehicles. If the car is traveling at 100km/h and is approaching another car at a relative speed of 20km/h, throttle-controlled deceleration begins at a distance of about 85m. Deceleration continues until the speeds of the two vehicles are matched at 80km/h and a 45m following distance is established. If the relative speed of the two vehicles is excessively high, that is, if the car is approaching another car too quickly to be handled by throttle control, the throttle will close and an alarm buzzer will sound to signal the driver to brake.

If the preceding car moves out of the way, the system returns control to the cruise control and the speed returns to the preset value.

This vehicle distance interval control system supplements the capabilities of conventional cruise control. We believe that the system will find wide acceptance among drivers because the two systems work well together, and because operation is substantially the same as that for a

cruise control. In the future, smoother control will be achieved through closer integration with the cruise control system. These improvements will require continued advances in the technologies for sensing the vehicle environment. □

A Drowsiness Detection System

by Kenji Ogawa and Mitsuo Shimotani*

Systems that detect when drivers are becoming drowsy and sound a warning promise to be a valuable aid in preventing accidents. This article reports on a drowsiness detection system developed at Mitsubishi Electric. The system analyzes facial images of the driver to determine blinking behavior, which it uses as a measure of driver alertness. An accurate realtime drowsiness detector prototype was manufactured and tested in actual vehicles.

Waning Alertness Experiments

We studied the relationship between alertness and blinking behavior by testing ten subjects in the driving simulator illustrated in Fig. 1. The subjects had to drive through nighttime freeway scenery, and while doing so, underwent two tests. The first, a tracking test, was to control the steering and accelerator to keep a cursor aligned with the image of the preceding vehicle. The second, a reaction time test, was to press a button on the dash the moment a red square appeared on the screen.

A VCR recorded changes in blinking behavior as the subjects grew drowsy. Also monitored were the subjects' brainwaves, eye movements and other physiological indicators. The subjects evaluated their own subjective state of alertness by pushing buttons for slightly sleepy, moderately sleepy and very sleepy. The results of the reaction time test were also recorded.

Test Results and Analysis

We tested ten subjects (eight male, two female) ranging in age from 21 to 59. Nine of the ten subjects experienced waning alertness.

We analyzed the relationship between alertness and blink duration. Fig. 2 shows the relationship between decreasing alertness and blink duration. For each minute, the figure shows a histogram for various blink durations, reaction times and subjective drowsiness evaluations. Long blink durations became more frequent as the subjects began to report feeling drowsy. At the same time, alertness waned, causing reaction times to extend to 2s and longer. Table 1

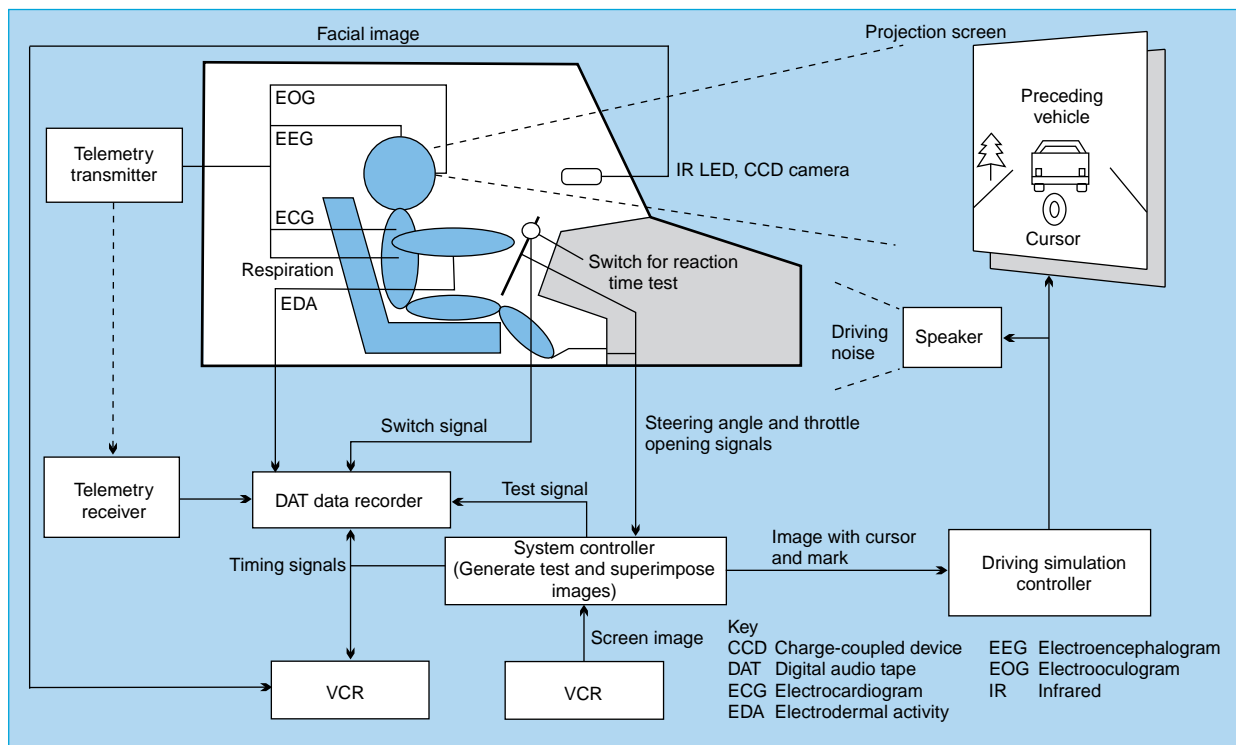


Fig. 1 The laboratory test apparatus.

*Kenji Ogawa is with the Himeji Works and Mitsuo Shimotani with the Industrial Electronics & Systems Laboratory.

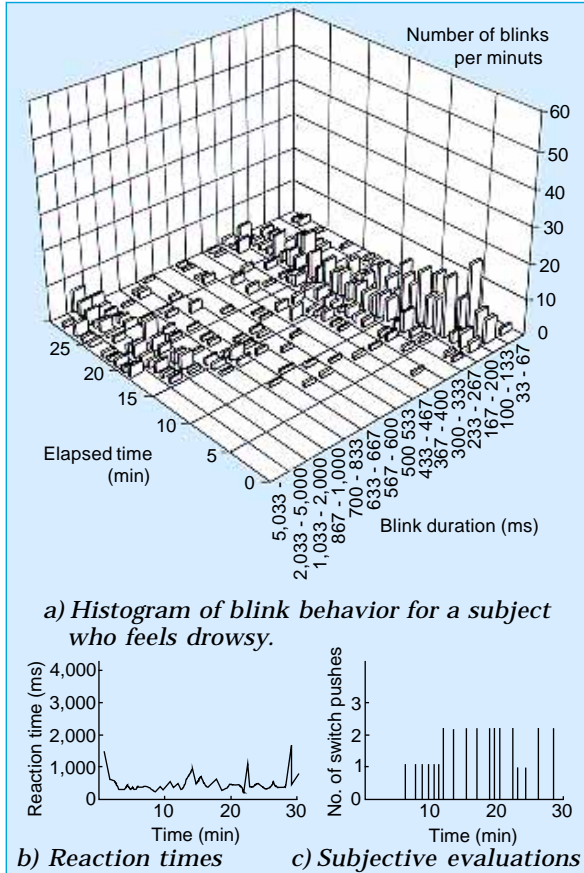


Fig. 2 Results of analysis for subjects

lists the test data, from which we drew the following conclusions:

The average blink duration for alert subjects varies with the individual. Long blink durations of a half-second or more correspond to subjective evaluations of slightly or moderately sleepy. The one subject who remained completely alert recorded no blink durations over a half-second. Blink durations of a half-second or longer were always present when reaction times over two seconds were recorded.

Alertness Inference Algorithm

Knowing that average blink durations differ for alert subjects, and that longer blink durations are associated with decreasing alertness, led us to develop an alertness inference algorithm based on the following principles: (1) Statistics on blink duration are collected when the driver

Table 1 Elapsed Time Until Various Drowsiness Indications (min)

Subject		Blink duration over 0.5s	Subjective evaluation			Reaction time over 2s
Sex	Age		Slightly sleepy	Mod. sleepy	Very sleepy	
M	21	10	11	13	33	22
M	25	7	10	15	19	16
M	29	10	9	12	—	12
M	37	9	5	9	13	12
M	43	13	18	34	37	50
M	44	—	8	12	18	44
M	45	—	—	—	—	—
M	59	5	3	8	—	12
F	23	25	56	—	—	—
F	29	11	5	11	31	35

is assumed to be alert, and a threshold for judging long blink durations is established. (2) The degree of alertness (α) is periodically calculated as follows:

$$\alpha = \frac{\text{number of long duration blinks}}{\text{total number of blinks}} \dots\dots\dots \text{(Eq. 1)}$$

The driver is judged drowsy when α falls below a specified threshold.

Blink Detection

We used a small CCD camera mounted in the vehicle instrument panel to capture images of the subject's face while driving. We had to surmount several hurdles in developing an effective method to measure blink duration. The first was dealing with rapid changes in solar illumination during daytime driving. Sometimes a driver's face is illuminated by direct sunlight; sometimes parts of the face are shadowed by pillars or a sun visor; and these illumination patterns change quickly. Second, artificial illumination must be provided in tunnels and during nighttime driving.

The nighttime illumination problem was resolved by using an invisible infrared light source. We rejected this approach for daytime use because the great number of LEDs required to provide appropriate daytime illumination lev-

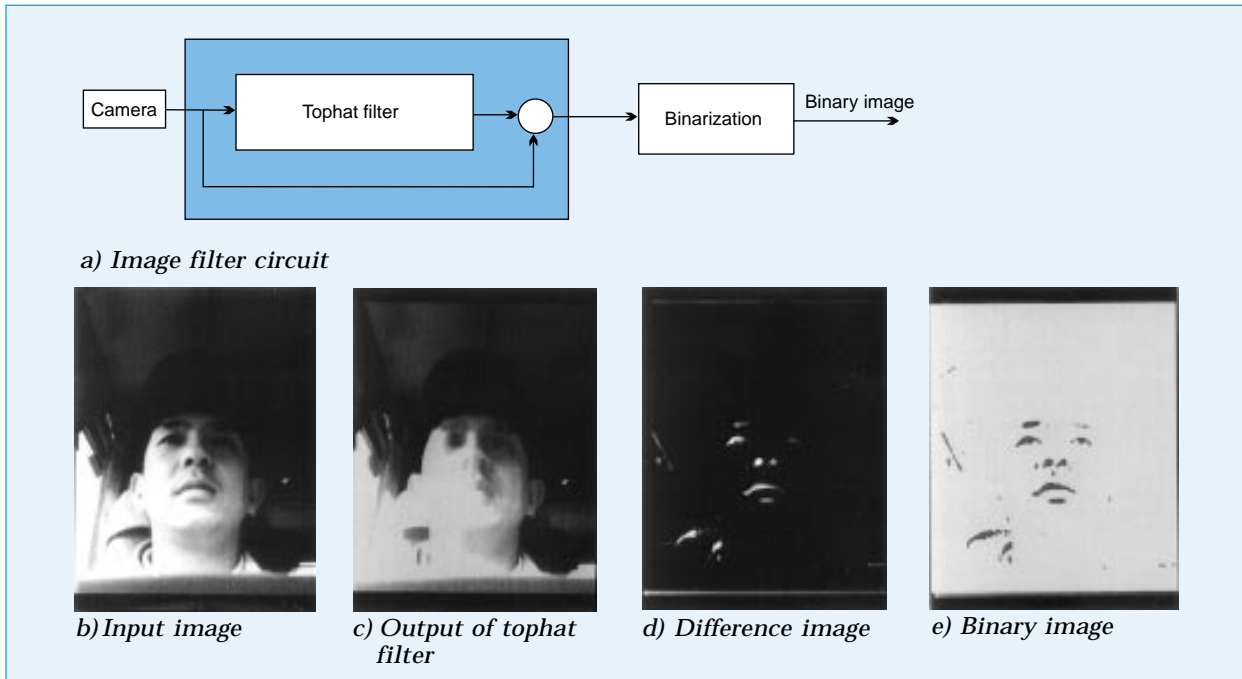


Fig. 3 Image filtering process.

els would be expensive, would increase power consumption and might present a potential vision safety hazard. Instead, we explored digital filtering methods that generate a reliable image of the driver's eyes from a facial image captured under variable daytime illumination.

DAYLIGHT BLINK DETECTION. Fig. 3a shows a block diagram of the image filtering system. First applied is a tophat filter that removes dark regions that are short in the vertical direction. When a tophat filter is applied to the camera image of Fig. 3b, the eyebrows, eyes and nostrils are removed, yielding the image of Fig. 3c. Fig. 3d, the difference between Figs. 3b and 3c, shows the eyebrows, eyes and nostrils. A binarization filter applied to Fig. 3d yields Fig. 3e. The filtering not only eliminates the shadowing visible in Fig. 3b but also eliminates hair, background and other unnecessary details.

The binary image is then analyzed to monitor blink duration. Fig. 4a shows a steeper inclination of the eye corners with the eyes open than in Fig. 4b when the eyes are closed. Measuring this quantity gives a robust indication

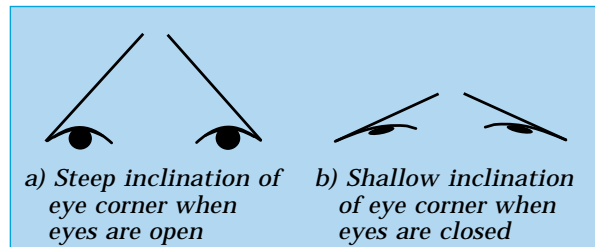


Fig. 4 Method of daytime blink detection.

of the state of the eyes that is largely unaffected by changes in distance between the driver and camera.

NIGHTTIME BLINK DETECTION. Under low-illumination conditions, the reflection from the retina can be monitored to determine whether the eye is open or closed. Infrared LEDs aligned with the optical axis of the camera lens illuminate the driver's face (Fig. 5a). Infrared light enters the pupil and is reflected by the retina (Fig. 5b). This reflection is captured by the camera (Fig. 5c). The driver's face is dim, but the reflection from the pupil is bright. These bright reflections are absent when the eyelids are

closed. Low-intensity illumination is sufficient to detect these reflections.

By using blink duration as a indicator of driver alertness, the electronic equipment and algorithms presented in this report provide a foundation for manufacturing accurate and inexpensive drowsiness detectors. Future studies using vehicle-mounted prototypes will be used to study the blink behaviors of a larger sample as well as methods to support driver alertness. □

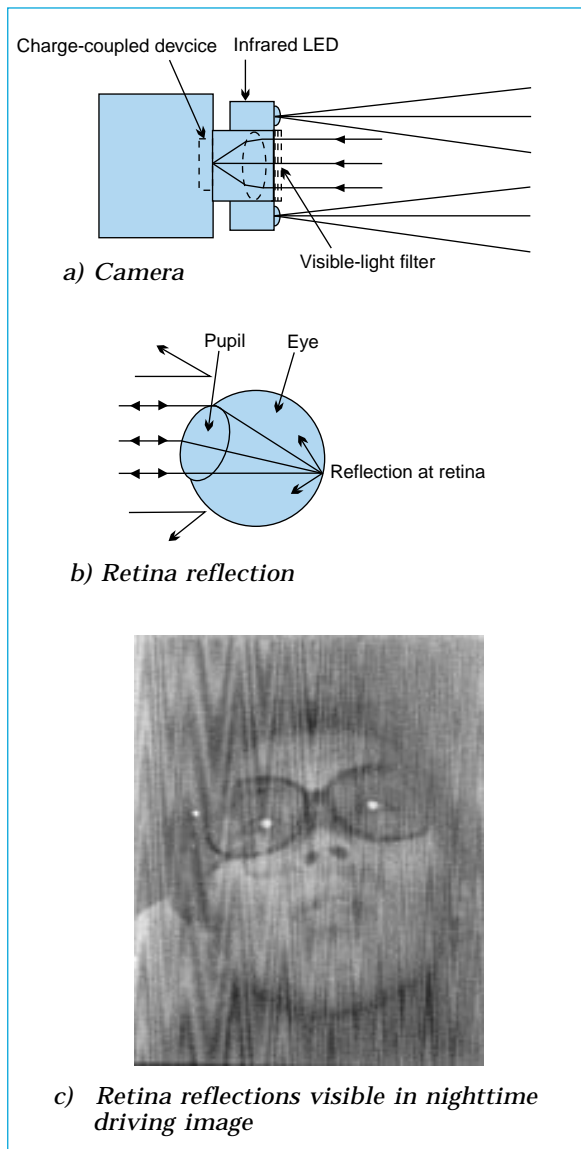


Fig. 5 Method of nighttime blink detection

Motor-Drive Control Technology for Electric Vehicles

by Kazutoshi Kaneyuki and Dr. Masato Koyama*

Because they emit no exhaust gases, electric vehicles are increasingly attractive to governments and industries concerned with reducing atmospheric pollution. Mitsubishi Electric is applying its experience in electric motors and power electronics to develop drive systems for high-performance electric cars. This report describes recent developments in this area.

Traction Motors

We chose three-phase cage-rotor induction motors as best suited to electric vehicle drive applications. Induction motors are cost-effective, and are suitable in terms of size and weight, speed of rotation, efficiency, controllability and reliability. The durable rotor and high-speed operation under easily implemented field-weakening control enable the use of large reduction gear ratios that limit maximum torque requirements, allowing the incorporation of smaller motors driven by compact low-current inverters.

We selected water cooling over forced-air motor cooling because it offers superior cooling performance and supports compact, lightweight motor designs. Our analysis showed that use of water cooling permitted weight reduc-

tions of 20% and size reductions of 30% as compared to forced-air designs, while the power consumption for cooling dropped by 75%. Use of a single water-cooling system for the motor and the inverter's power module permitted further size reductions. Another advantage of water cooling is that the motor can be sealed more completely, which facilitates dust- and weather-resistant design.

Fig. 1 shows the construction of the induction motor that we developed for this application. The stator features a low-loss core material and highly heat-resistant insulators. High-density windings are used with lightweight housing materials that yield motors one-third smaller and lighter than general-purpose induction motors of the same output. The water-cooling unit was placed on the upstream side of the motor.

Motor-Drive Electronics

The drive electronics consist of an inverter that drives the motor and a controller that controls the inverter's output voltage waveform. The system was specially developed to satisfy the specific requirements of electric vehicles.

An inverter generally includes power devices, a drive circuit, a protection circuit, a smoothing condenser and a snubber circuit. We simplified the inverter by using high-performance intelligent power modules (IPMs) based on in-

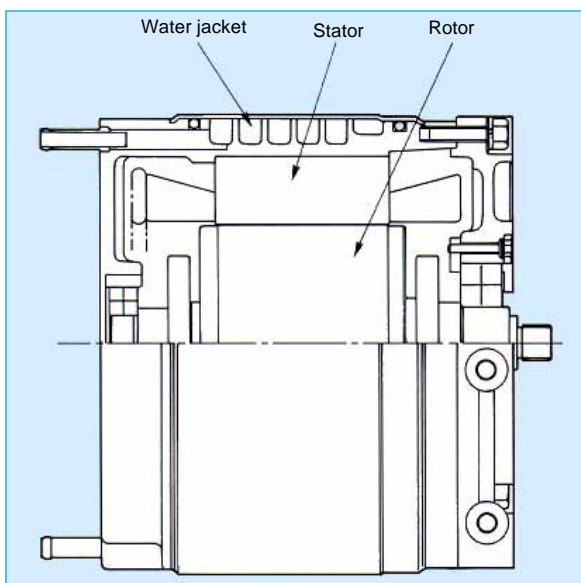


Fig. 1 Construction of an induction motor for electric vehicle use.

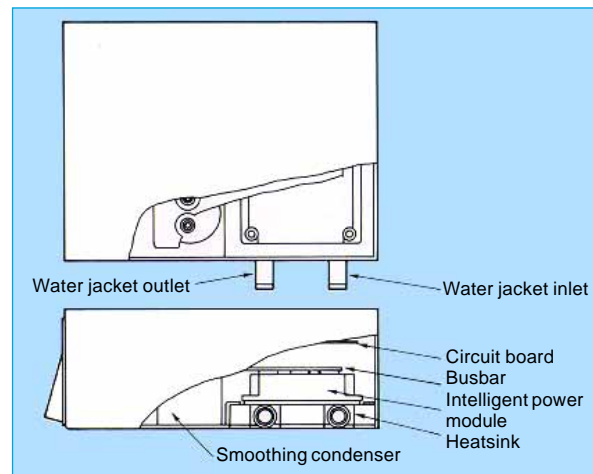


Fig. 2 Construction of the controller.

*Kazutoshi Kaneyuki is with the Himeji Works and Dr. Masato Koyama with the Industrial Electronics & Systems Laboratory.

sulated-gate bipolar transistors (IGBTs) that integrate the power devices, drive circuit and protection circuit. We eliminated the snubber circuit by positioning the flat busbar and smoothing condenser to maximize noise canceling effects. We were also able to substantially reduce the size of the IPM by closely matching the characteristics of the motor and IPM.

The controller includes a torque command processor that computes the optimum torque command for current driving conditions, and a motor control unit that supplies the three-phase motor-drive voltage for maximum efficiency based on the torque command, voltage and current values. The controller is implemented as a single-chip microprocessor with motor and control constants, and other parameters carried in flash memory. This design allows the use of a standardized controller in a variety of applications.

Taken together, these design choices allowed us to reduce the size of the drive electronics by 50% and the weight by 45% as compared to controllers employing discrete IGBTs.

Highly Efficient, Fast-Response Vector Control Technology

We employed a proprietary slip-frequency-controlled vector-control algorithm to implement fast-response vector control for the induction motor. This method, which employs a model of the primary circuit of the induction motor, infers the secondary-circuit flux vector from the motor speed and primary current, then conducts feedback control on the motor’s magnetizing current and torque current using the d-q coordinates that rotate synchronously with the flux vector. This design results in smoother motor operation with fast torque-control response at speeds ranging from a standstill to the motor’s maximum rating. The vector-control algorithm has been proven in induction motor drive systems for steel rolling mills and numerous other applications requiring precise torque control and fast response.

The motor-drive conditions for maximum efficiency are determined as follows. From the motor circuit equation, we know that the ratio of the q-axis component of the secondary current (i_{qr}) to the secondary flux vector amplitude (ϕ_{dr}) matches a specific variable determined by the motor constants and the primary frequency. We also know that the induction motor output torque (τ_m) is proportional to the product of i_{qr} and ϕ_{dr} . Now, while satisfying the above maximum efficiency conditions, we can select the

i_{qr} and ϕ_{dr} which suit the torque command.

Fig. 3 shows the block diagram of a vector control system implementing this algorithm. Commands for i_{qr} and ϕ_{dr} are computed based on the maximum efficient drive conditions and the torque command determined by the flux and current command calculator. The secondary flux vector estimator and primary voltage command calculator then perform vector control to ensure that i_{ds} and i_{qs} follow the corresponding commands.

Fig. 4 compares the efficiency of the new vector control system at various torque and speed ranges against that of a conventional control system. The efficiency improvement is espe-

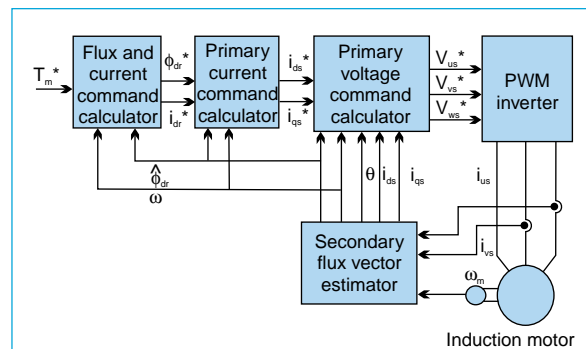


Fig. 3 Block diagram of a highly efficient vector control system.

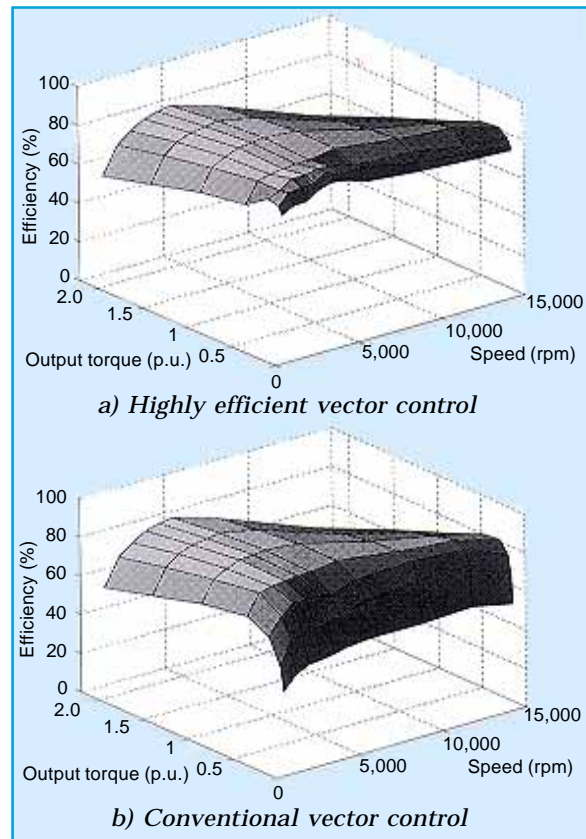


Fig. 4 Motor efficiency curves.

cially pronounced in the low-torque range, where an improvement of 35 percentage points was recorded. Since vehicles are frequently operated in the low-torque range, this improvement promises to bring a significant increase in cruising range. High efficiency means that less power is dissipated in the motor as heat, which permits higher motor output and smaller motor dimensions.

Sensorless Speed Control Technology

Use of vector control makes it possible to realize fast-response torque-control characteristics, however a weakness of vector control is that it requires motor speed information, which is generally provided by an external sensor. Numerous researchers are investigating sensorless vector-control solutions [that promise greater accuracy and reliability]. Recent advances in microprocessor performance and control technology have led to sensorless vector-control systems with improved performance that are now being applied to general-purpose inverter-controlled motor-drive systems.

However another problem—poor torque linearity during low-speed regenerative braking—has remained. In practical terms, this means that the control system is unable to apply sufficient regenerative braking torque at low speeds.

We addressed this issue by developing a secondary-circuit flux vector identifier employing model referenced adaptive control (Fig. 5). This identifier matches the secondary flux vector (computed using a reference model of the induction motor’s primary circuit) to the secondary flux vector identifier value (computed from the secondary-circuit model) using an adaptive algorithm to adjust the motor speed (ω_m) to the value required by the secondary circuit model.

By experimenting with the adaptive algo-

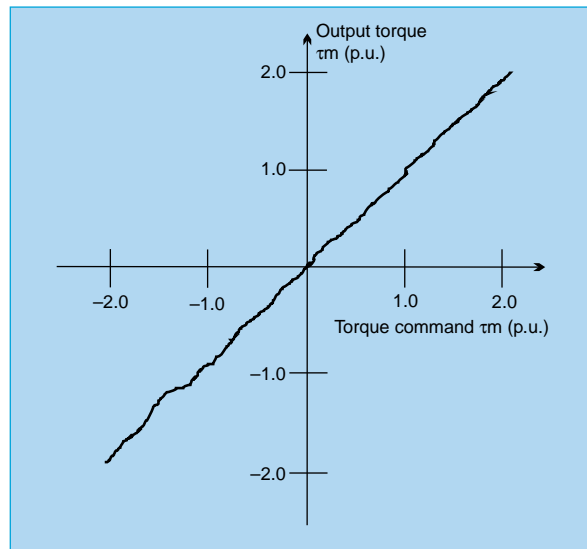


Fig. 6 Torque control characteristics at 2% of rated speed on a 200V, 60Hz, 1.5kW test motor.

rithm, we were able to improve the accuracy of secondary flux vector prediction under low-speed regenerative conditions. By replacing the secondary flux vector estimator in Fig. 3 with this identifier, we achieved the required performance of a sensorless vector-control system. Fig. 6 shows the torque-control characteristics of this system under low-speed regenerative operation, indicating that torque linearity is maintained.

Electric vehicles promise to lower atmospheric pollution by dramatically reducing vehicle emissions. Ongoing industry-wide R&D will gradually bring the improvements in performance, cost and convenience required for wide acceptance of this modern transportation technology. Mitsubishi Electric plans to continue researching and developing motor-drive and other related technologies for this application. □

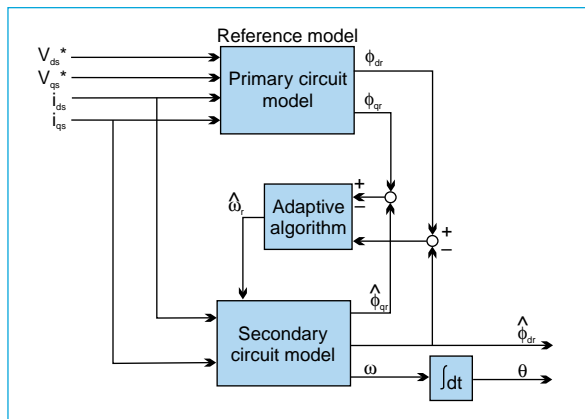


Fig. 5 Block diagram of a secondary flux vector identifier.

An Electric Power-Steering System

by Takayuki Kifuku and Shun'ichi Wada*

Electric power-steering systems for larger vehicles have not been mass produced because the high-output motors required for this application add inertia and friction that cause an unacceptable loss of road feel. This report introduces a new motor control system that eliminates this problem.

Problems in High-Output Electric Steering Systems

When a high-output electric motor is used to provide steering assistance, the motor's large inertia and friction torque become significant with respect to the tires' self-aligning torque. The steering wheel return is sluggish and road feel suffers. We addressed this problem in two ways: by minimizing the motor's friction torque and by developing methods to compensate for the motor's inertia and friction torque.

A large motor also causes heat dissipation problems in the drive circuitry due to the higher armature current. We redesigned this circuit for lower loss.

Friction Torque Reduction

There are two main sources of friction torque in the permanent magnet DC motors used in the application: mechanical losses in brushes and bearings, and magnetic losses. Larger motors require bigger brush-to-commutator contact areas to maintain low electrical resistance, and the magnetic flux density is also higher. Both of these losses therefore increase with the motor output, causing larger friction torques.

Use of magnetic field analysis to optimize the core design can reduce the magnetic losses. Fig. 1 shows magnetic loss before and after this optimization was carried out, both calculated and measured. A reduction of better than 60% was achieved.

Compensation for Motor Inertia and Friction Torque

As shown in Fig. 2, the desired motor current is calculated as the arithmetic sum of the power-assist current, and inertia, damping and friction compensation currents. The motor control circuit applies this current, adjusting itself to

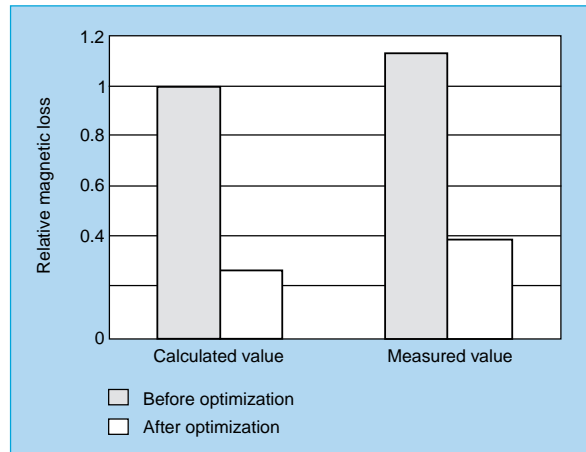


Fig. 1 Magnetic loss.

provide precisely the indicated value.

The steering assistance control determines the driver's static steering effort. The output of a torque sensor is phase compensated and the characteristics of Fig. 3 are applied to give the driver positive road feel at higher speeds.

The motor operation is governed by

$$K_T \cdot I_a = T_L + J_M \cdot (d\omega_M/dt) + D_M \cdot \omega_M + F_M \cdot \text{sgn}(\omega_M) \dots\dots\dots (\text{Eq. 1})$$

where K_T is the motor torque constant, I_a is the armature current, T_L is the load torque, J_M is the motor inertial moment, ω_M is the motor angular velocity, D_M is the motor's viscous friction coefficient and F_M is the motor friction torque.

For the inertia compensation to cancel out the disturbance torque caused by the motor inertial moment (J_M), the motor inertia compensation current (I_j) must satisfy

$$I_j = K_j \cdot (d\omega_M/dt) \dots\dots\dots (\text{Eq. 2})$$

where K_j is a constant representing the inertia compensation gain.

While inertia compensation improves steering responsiveness, it also causes damping problems that affect steering stability, especially at highway speeds. The required damping compensation current (I_D) is given by

*Takayuki Kifuku and Shun'ichi Wada are with the Himeji Works.

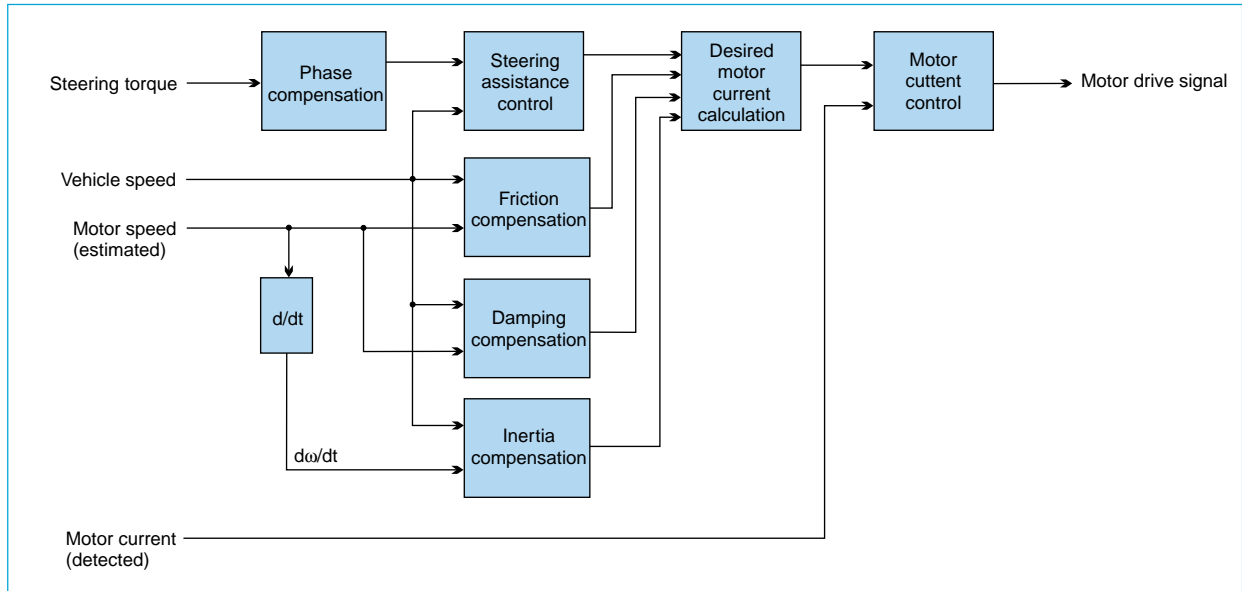


Fig. 2 A block diagram of the electric power steering system.

$$I_D = -K_D \cdot \omega_M \dots \dots \dots \text{(Eq. 3)}$$

where K_D is a constant representing the damp-
ing compensation gain.

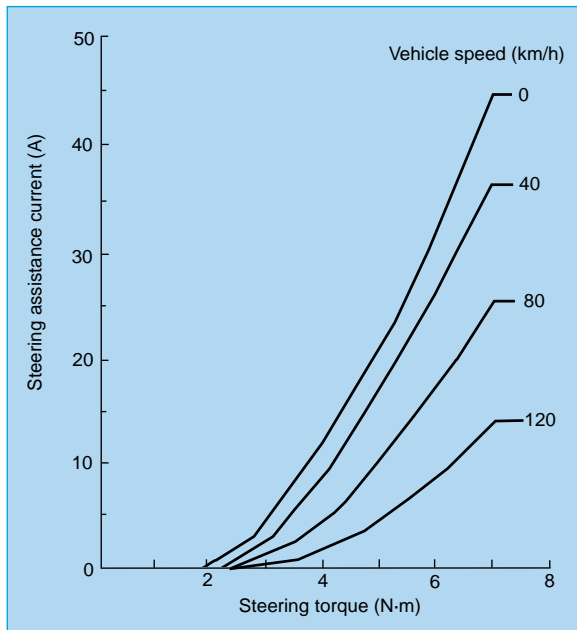


Fig. 3 Steering torque vs. steering assistance current curves.

The motor friction compensation current (I_F) is given by

$$I_F = K_F \cdot \text{sgn}(\omega_M) \dots \dots \dots \text{(Eq. 4)}$$

where K_F is a constant representing the friction compensation gain.

The inertia, damping and friction compensation all vary as a function of ω_M , so some means of detecting this quantity must be provided. Since ω_M is proportional to the motor's induced voltage, we can determine ω_M from the induced voltage and substitute, allowing us to implement the above control functions without the use of an external sensor.

Reduction of Motor-Drive Circuit Loss

The motor-drive circuit consists of power MOSFETs in an H bridge circuit that is driven by pulse width modulation (PWM) over a 20kHz carrier. Fig. 4 shows two PWM-driven H bridge circuits. Current control is simpler for the circuit of Fig. 4a while the loss of the circuit of Fig. 4b is smaller. We obtained the advantages of both by switching between the two configurations as appropriate.

Fig. 5 shows the motor current control sys-

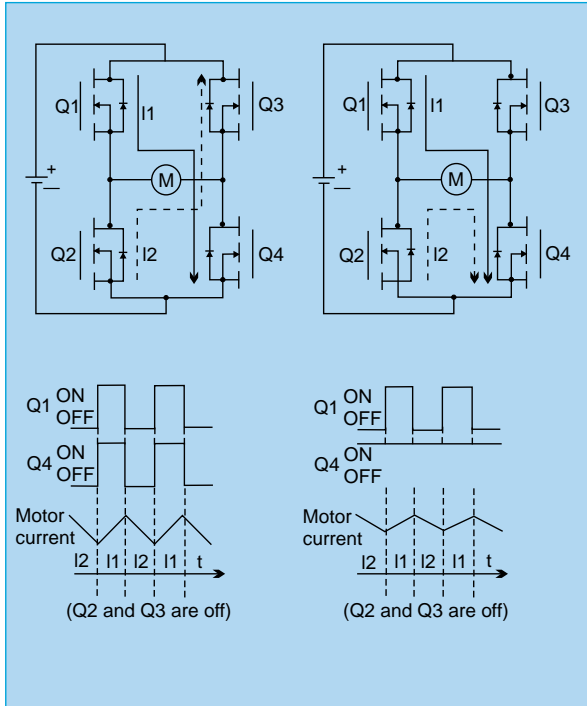


Fig. 4 PWM driven H bridge circuits.

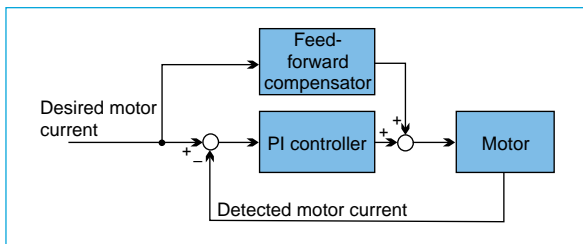


Fig. 5 A block diagram of the motor current control system.

tem. A power inertia (PI) controller implements feedback control while feed-forward control is implemented by a composite approach. Feed-forward control improves the responsiveness of the motor current and suppresses the ripple currents associated with switching between the two PWM methods.

Results

Fig. 6 shows the (steering angle/torque) frequency characteristics measured by sweeping the steering frequency with the vehicle traveling at 50km/h. Applying inertial compensation

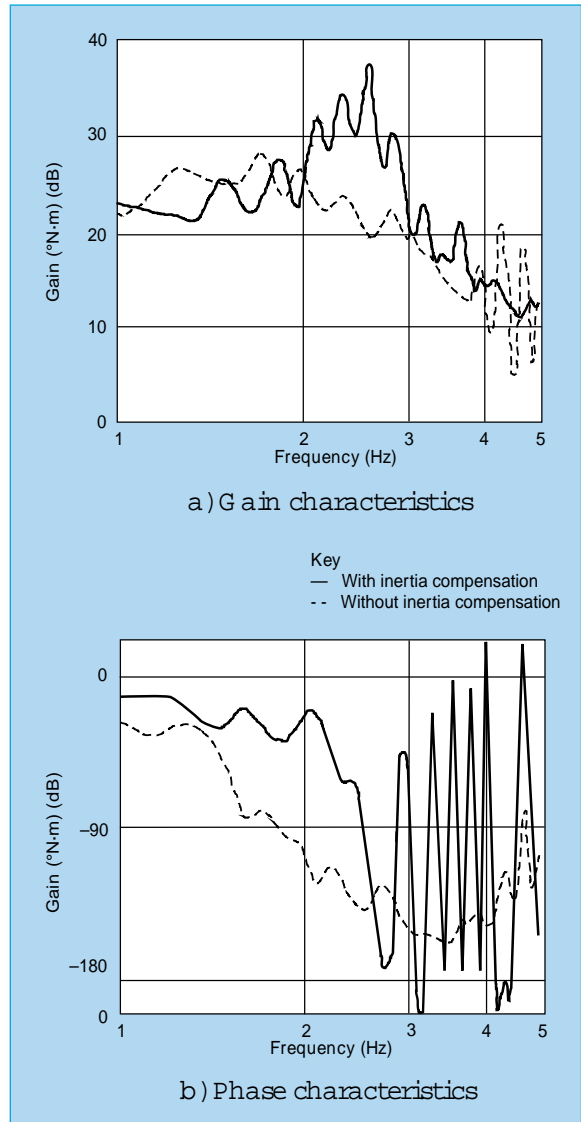


Fig. 6 Measured steering angle/steering torque frequency characteristics.

causes a phase lead in the 1~ 3kHz region that indicates enhanced responsiveness. Fig. 7 shows how the steering wheel returns from lock when released at a vehicle speed of 10km/h. The wheel returns to center smartly when friction compensation is applied.

Through use of the inertia, damping and friction compensation technologies presented here, electric power-steering systems that save space

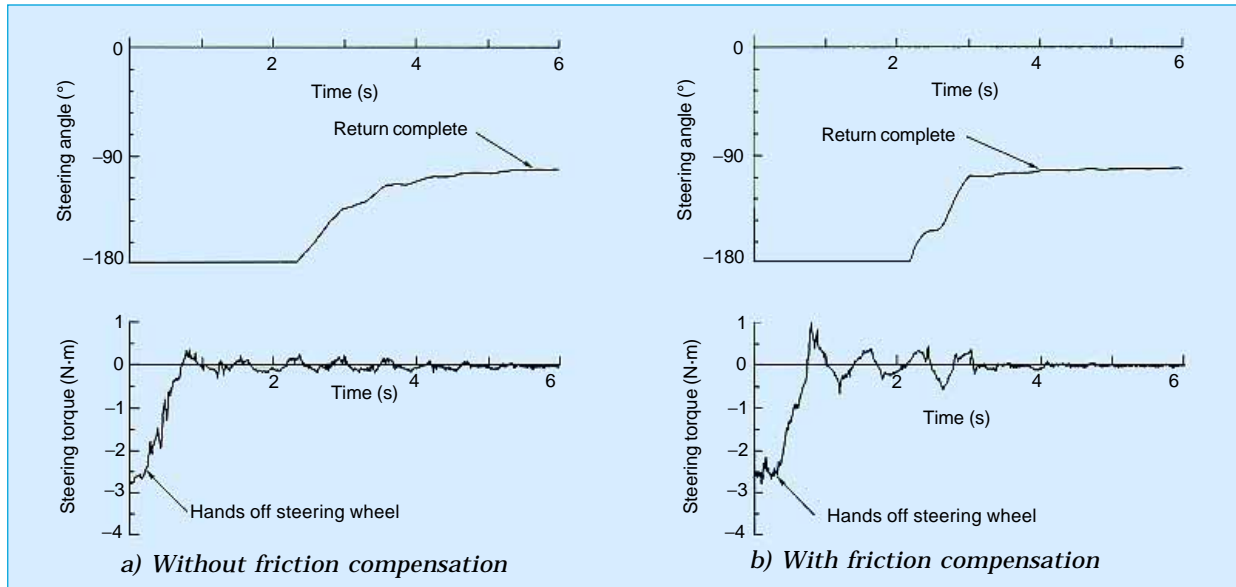


Fig. 7 Measured steering wheel return at low vehicle speed.

and improve fuel economy can be applied to large cars without sacrificing road feel. The authors would like to acknowledge the generous cooperation of the many people who have contributed to this project. □

Technologies for Gasoline Engine Control and ECU Miniaturization

by Yoshinobu Morimoto and Takanori Fujimoto*

Car electronics have helped car makers satisfy emission requirements and boost engine performance. Their role is expanding to include additional functions and convenience features such as customizing car operation to individual drivers. This report surveys trends in engine control technology and engine control units.

Engine Control Systems

Fig. 1 illustrates requirements for engine performance and engine control systems.

Mitsubishi Electric has developed a knock-control system and implemented it in an 8-bit microprocessor. The low-cost system improves engine operating characteristics.

Larger engines of over two liters are starting to incorporate lean-burn systems that keep the gas-air mixture as lean as possible for better fuel economy. Mitsubishi Electric and Mitsubishi

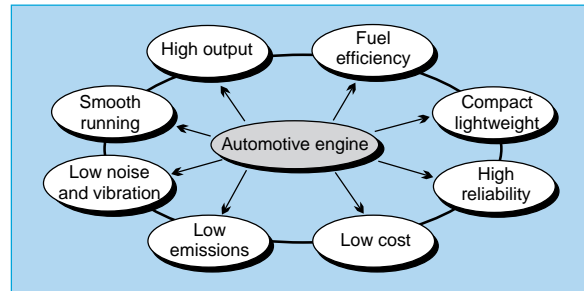


Fig. 1 Goals of automotive engine design.

Motors have jointly developed a linear airflow sensor and a control system that respond to fluctuations in engine speed. The corporation has developed improved airflow feedback control and an exhaust gas recirculation (EGR) system with feedback control that help meet strict new emission control standards.

The corporation has also developed sophisti-

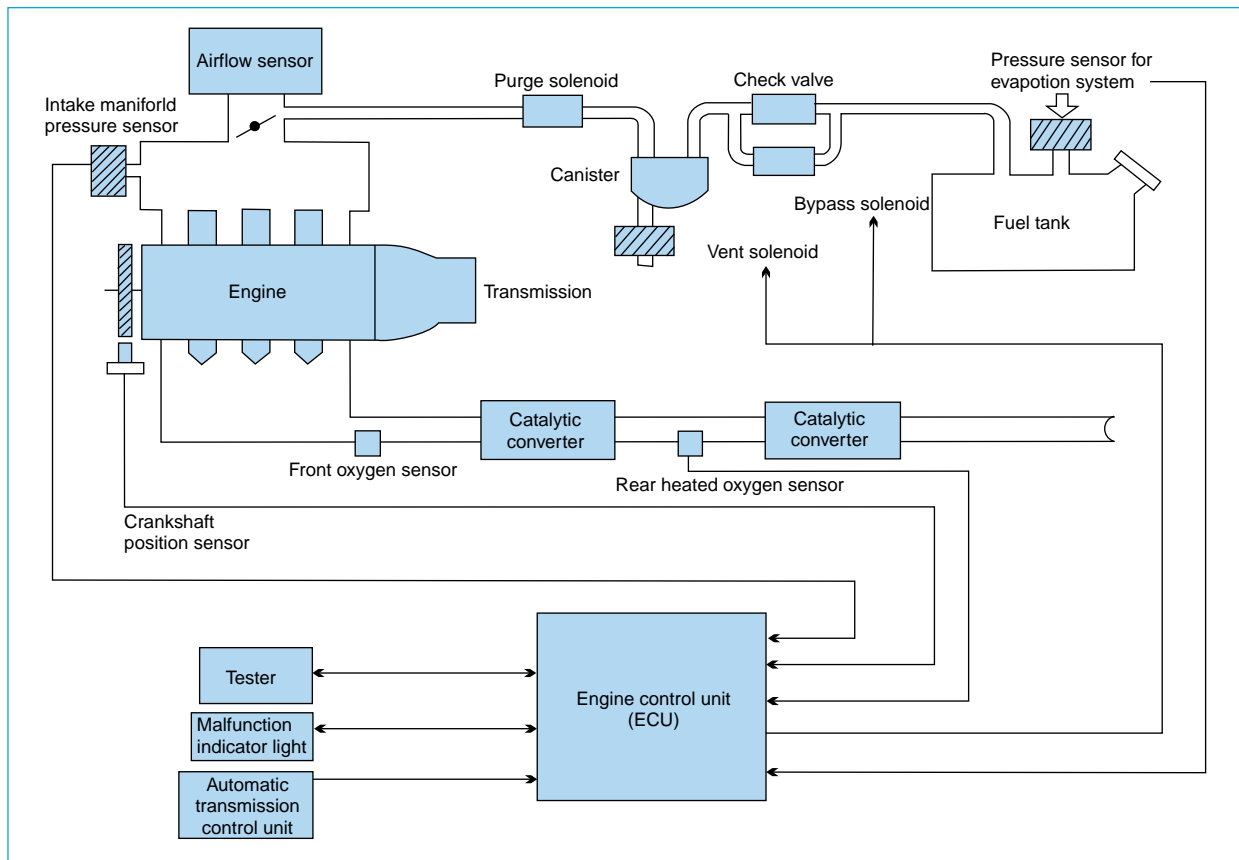


Fig. 2 Mitsubishi Electric's OBD-II onboard diagnostic system.

*Yoshinobu Morimoto and Takanori Fujimoto are with the Himeji Works.

cated on-board diagnostics that detect misfires by fluctuations in engine speed. This technology has been incorporated in production vehicles since 1994. Fig. 2 shows an engine control system employing these new diagnostics.

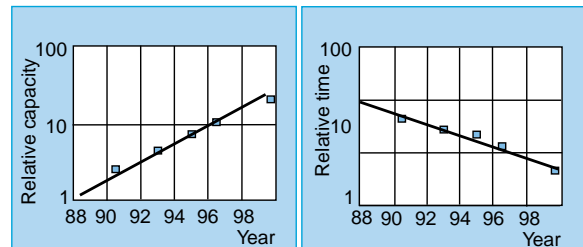
Current electronic engine control systems limit engine torque during automatic transmission shifts for smoother shift transitions. More recently, data from the engine is being used to optimize the automatic transmission shift patterns. Mitsubishi Electric has developed and is mass producing engine control units (ECUs) that integrate engine and automatic transmission control for compact and subcompact cars.

Engine Control Technology

More sophisticated control programs are being developed to further improve engine performance and fuel economy. Executing these programs requires high-performance ECUs. Since ECU performance is limited by microcomputer performance, Mitsubishi Electric has developed high-performance microcomputers for ECU applications. ECU developers are rapidly changing over from 8- to 16-bit microprocessors that offer faster computing and larger memory capacity. Fig. 3 shows trends in ECU microcomputer arithmetic speed and memory capacity. Table 1 lists typical microcomputer specifications. Microcomputers with a large on-chip flash EEPROM are being utilized to support shorter development time.

Software Development

Manufacturers have developed engine control software in assembly language due to limitations on microcomputer speed and memory capacity. With the larger memory capacities available in 16-bit microcomputers, software



a) Memory size

b) Speed for 16 x 16 bit multiplication

Fig. 3 Trends in microcomputers for automotive applications.

Table 1 Typical specifications for ECU Microcomputers

Architecture	16 bit		
	8 bit	62kB	92kB
OTP ROM	60kB	62kB	92kB
RAM	1.5kB	2kB	3.25kB
Speed for 16-bit multiplication	7.8µs	2.3µs	2.4µs
ADC (bits x channels)	10 x 12	10 x 8	10 x 16
Timer channels	24	13	23
Serial communication interface	2	2	3
Package	100-pin QFP	84-pin PLCC	136-pin QFP

development in the C language is growing more common. Mitsubishi Electric has developed optimized C compilers and program design guidelines that result in compact executable code just 1.3 times the volume of handcrafted assembly language.

ECU Hardware Technologies

Mitsubishi Electric is working to minimize ECU size through studies of both circuit design and production technology. ECUs must be com-

Table 2 Environmental Conditions at Several ECU Installation Sites

Location	Temperature	Water exposure	Vibration	Electromagnetic compatibility
Passenger compartment	-40 ~ 85°C	Negligible	4 ~ 5G max.	Protection required against noise from radio equipment
Engine compartment	-40 ~ 110°C	Complete waterproofing required	4 ~ 5G max.	Protection required against ignition and relay noise
Mounted on engine	-40 ~ 120°C	Water-jet protection required	35G max.	Protection required against ignition and relay noise

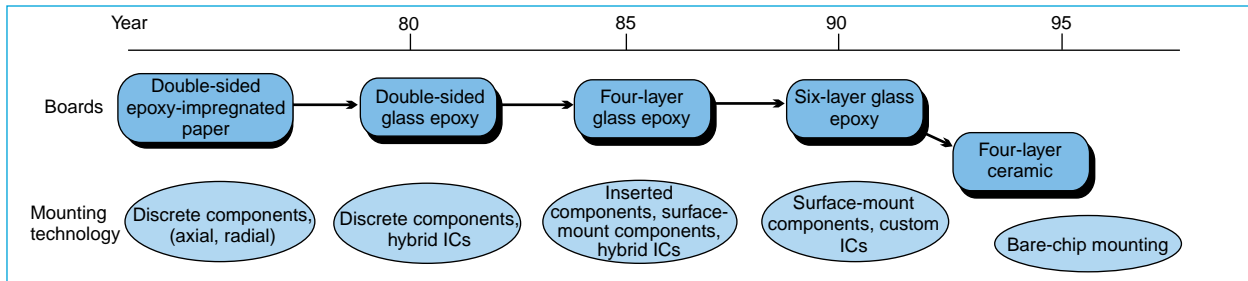


Fig. 4 Printed-circuit board and mounting technology for ECUs.

pact enough for space-efficient engine compartment mounting despite the large number of connections they require. ECUs must also resist temperature extremes, water and severe vibration—and they must be cost-effective. Table 2 lists environmental stresses associated with different mounting locations.

Mounting Technologies

Fig. 4 shows trends in printed circuit board (PCB) and component mounting technologies. ECUs designed to resist the harsh extremes of direct engine mounting will need to be fabricated by bare-chip mounting on a ceramic substrate.

Table 3 ECU Miniaturization Technologies

Component mounting
Exclusive use of surface mount components
High-density component placement, highly reliable soldering of QFP with 0.55mm lead pitch
High-temperature solder that endures engine-compartment heat cycling
Bare-chip mounting using die bonding and wire bonding technologies
Components
Small-outline packages such as QFPs with pin counts of 100 or more
Fine-line PCBs with conductor pitch of 0.25mm
Custom ICs that reduce component count
Development of power MOSFETs with low on-state resistance for reduced power dissipation
Case
High-density, high-pin-count connectors for 100 pins or more
Lightweight molded case
Water, shock and heat-resistant molding

Although much of the high-density assembly technology required for ECUs has already been pioneered for compact consumer electronic equipment, the operating environment and “mission-critical” nature of the ECU requires higher levels of reliability. Table 3 lists mounting technologies for ECU miniaturization.

Power dissipation is another obstacle to ECU miniaturization. The temperature difference between power devices in the ECU’s power supply and output circuits and the ambient temperature must be kept within 30°C. Highly efficient power MOS transistors with reduced dissipation offer a solution.

Another important issue is connector size. The complexity of ECUs with integrated automatic transmission control can require connection of as many as 110 to 120 conductors. ECU size reductions therefore await development of small, high-density connectors.

Mitsubishi Electric has adopted two approaches to ECU miniaturization. The first level takes maximum advantage of existing double-sided, surface-mounting technologies. The second level employs bare-chip mounting and wire bonding technologies to build ultracompact ECUs for direct engine mounting. Fig. 5 shows ECUs developed using these two approaches.

The final step in ECU miniaturization will occur when all necessary circuitry is implemented in a single silicon device that can be bare-chip mounted on a PCB. Achieving this level of integration will require development of standard circuits and continued integration of functions into custom ICs. ECUs comprising several custom ICs are currently being developed, and bare-chip mounting technologies will

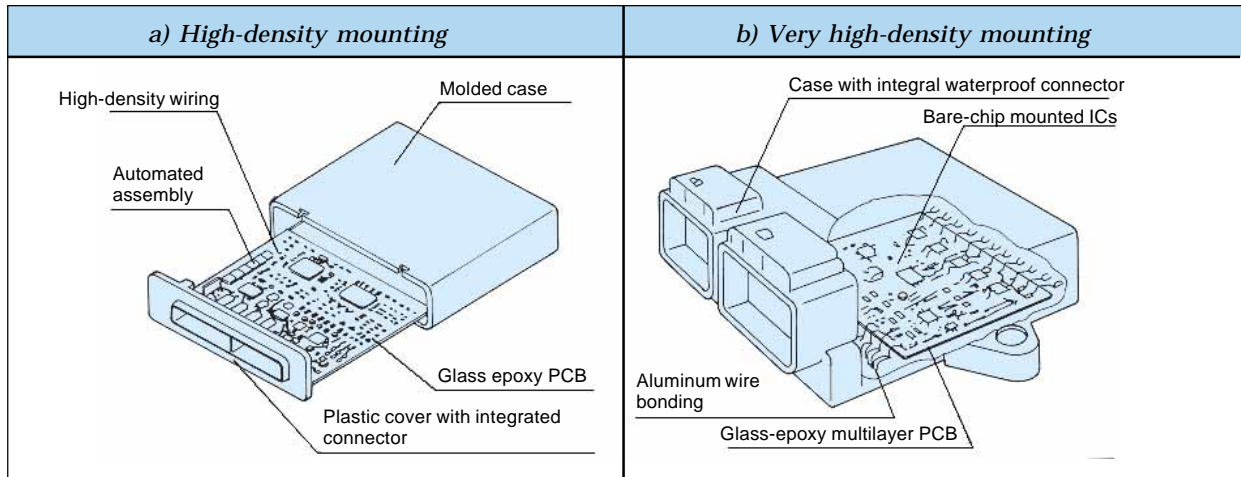


Fig. 5 ECU construction.

soon be ready for production.

Electronic technology contributes to cleaner vehicle exhaust and better fuel economy. Improvements in ECU design such as those described here will contribute to even better vehicle performance and reliability. □

Starting and Charging Systems for Fuel-Efficient Engines

by Toshinori Tanaka and Akira Morishita*

Demand for further reductions in automotive fuel consumption and emissions is expected to continue for the foreseeable future. This report describes the use of computer-aided engineering (CAE) and advanced materials to build small, lightweight starters and alternators. It also describes power generation control technology that reduces alternator loading.

Magnetic Flux Analysis

The copper windings and iron magnets are among the heaviest parts of motors and generators. Their weight can be reduced through improved electromagnetic design based on magnetic flux analysis.

In general, the size of a motor's electromagnetic components can be expressed as

$$D_a^2 L_c = K \cdot (1/g) \cdot (T/I) \cdot (1/\sqrt{R_s}) \dots \dots \dots \text{(Eq. 1)}$$

where D_a is the rotor diameter, L_c is the rotor length, K is a constant, g is the reduction gear ratio, T is the torque, I is the current and R_s is the internal resistance (a function of the output). T/I is referred to as the "torque gradient." This equation is used to determine the motor size once the motor's torque, output and reduction ratio are decided. New designs and technologies can influence the value of K , leading to smaller size and weight.

Mitsubishi Electric, for example, achieved a substantial reduction in starter motor size by introducing a six-pole magnetic starter motor with auxiliary poles (Fig. 1 (b)). The corporation recently introduced three-dimensional flux analysis to supplement conventional two-dimensional analysis (Fig. 2 (d)), and also lightened the solenoid that engages the motor by redesigning the plunger mechanism to match the plunger movement with the meshing of the pinion and ring gears.

Cooling Design

Fig. 3 shows the trade-offs between alternator output characteristics, permissible temperature rise and cooling noise. These trade-offs are important since the alternator rotates continuously while the engine is running and represents a sig-

nificant load. We began our redesign efforts by conducting an analysis of thermal stress and airflow characteristics. Since temperature affects the lifetime of the voltage regulator and rectifier, we redesigned the heatsinks for better cooling. We conducted an airflow cooling analysis of the alternator and then an overall study of cooling characteristics to develop a more effective cooling design. We also made models for visual studies of airflow characteristics (Fig. 4).

Structural Analysis

Another priority of our research was to address structural design issues. We analyzed the structure of many parts in the starter motor mechanism, optimizing shapes and reducing weight without sacrificing mechanical strength.

Plastic components have already proven thoroughly reliable for the starter reduction gear, pinion shift lever and switch plunger hook. We therefore studied using plastics for various other components as a means of reducing weight. Two components currently under study are the alternator pulley and the rear starter housing.

Plastics suffer the drawbacks of shock and wear resistance that are inferior to metals and they require special handling. Most housings are made of lightweight diecast aluminum. Further weight reductions may be achieved by using magnesium; however, problems related to mass production and cost remain to be solved.

Charging System Improvements

Control of alternator power generation offers another avenue to reduce the engine load. Here, we will introduce one solution; a load-response-controlled regulator developed at Mitsubishi Electric.

The alternator generates electricity when power is being used by the headlights and other electrical loads. Power generation draws on engine torque and can cause rough idling and even stalling. The load-response-controlled regulator maintains a stable load on the engine even when electrical loads fluctuate (Table 1). Stable alternator behavior allows the use of lower idle speeds, thus contributing to better gas mileage. Since headlamp output fluctua-

*Toshinori Tanaka and Akira Morishita are with the Himeji Works.

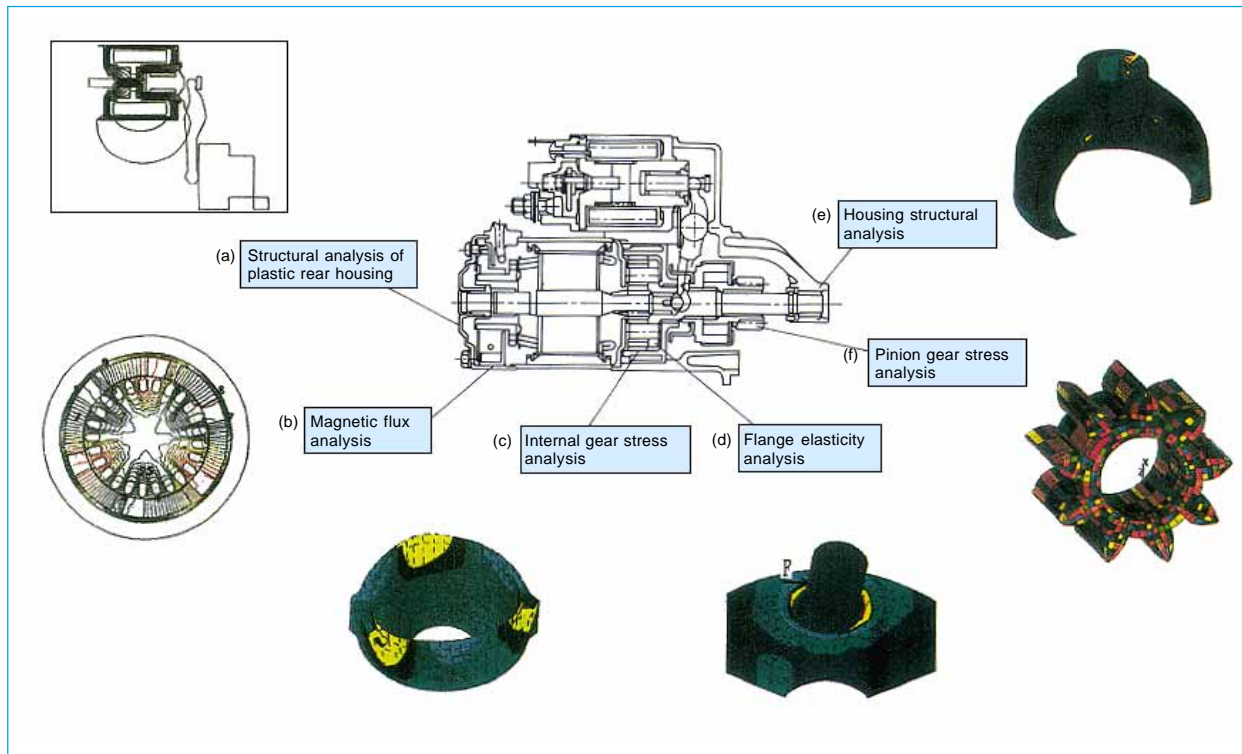


Fig. 1 Studies for starter motor improvement.

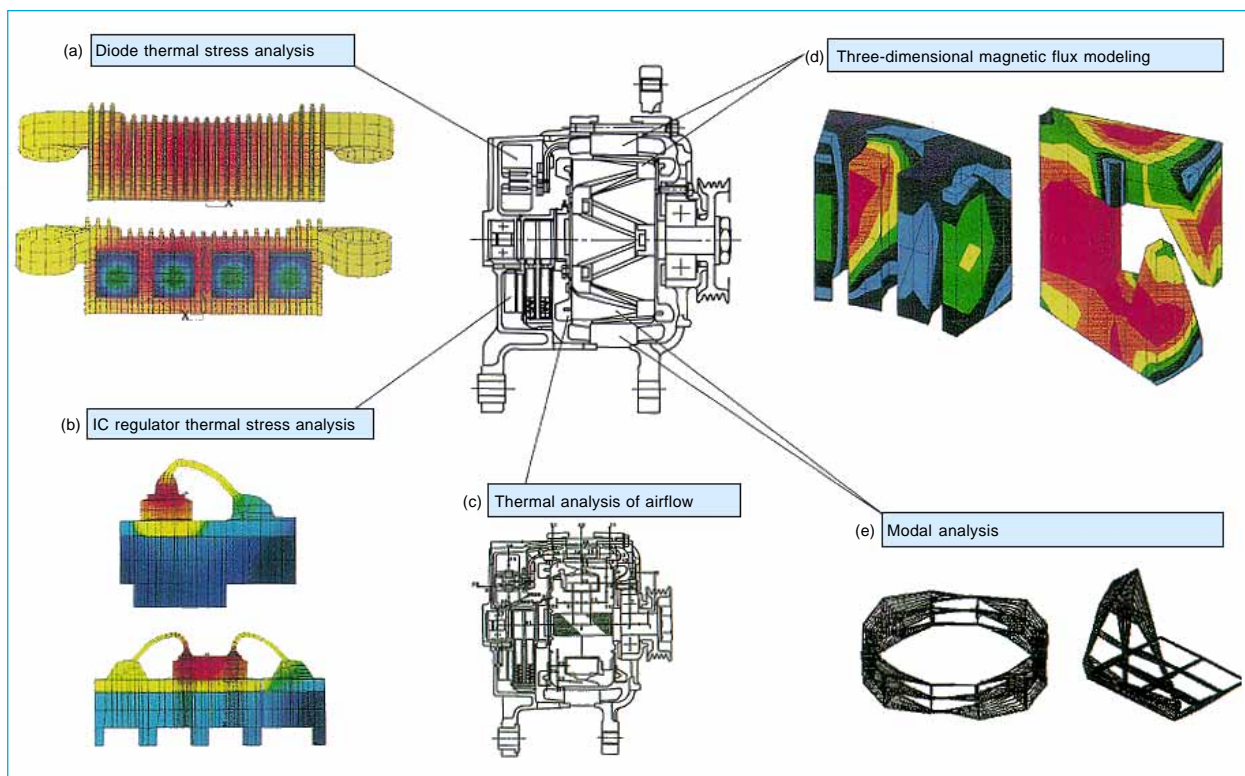


Fig. 2 Studies for alternator improvement.

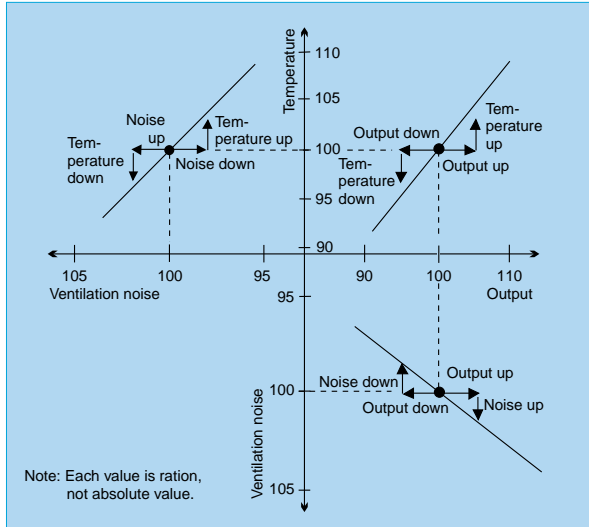


Fig. 3 Relationships between alternator output, temperature and ventilation noise (arbitrary units).

tions can occur as a side effect, the load-controlled regulator is disabled at cruising speeds. Table 2 shows the measured benefits of the load-controlled regulator. The idling speed can

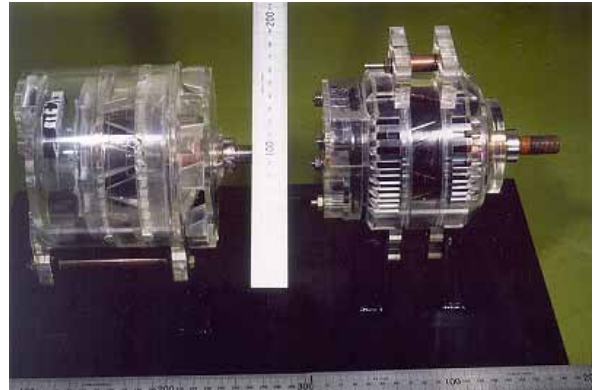


Fig. 4 A sample alternator with transparent housing.

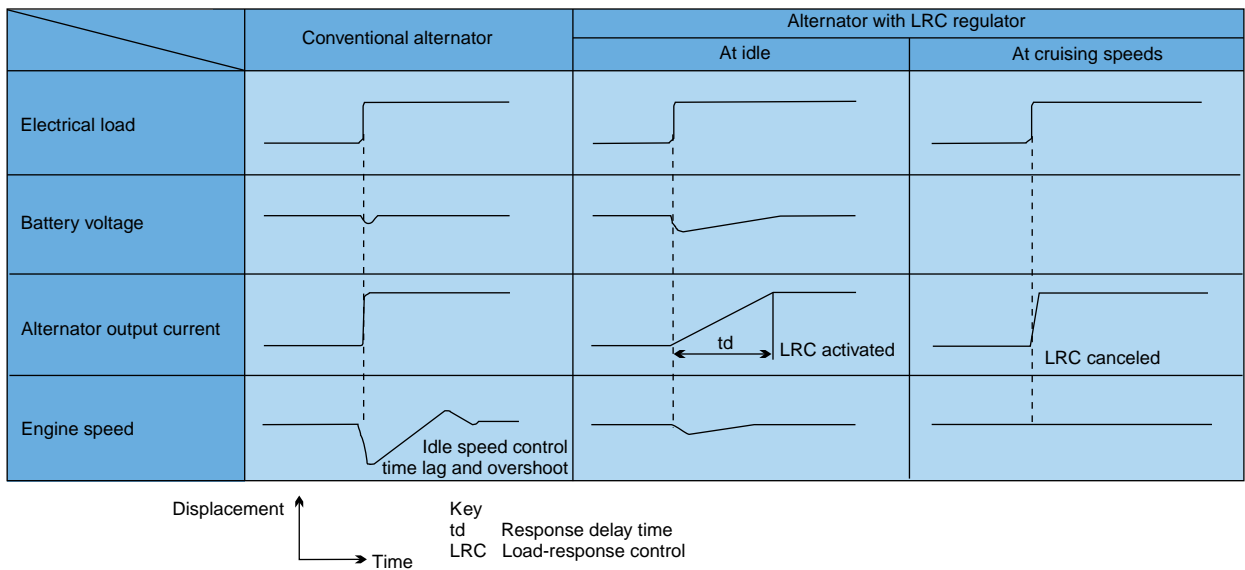


Table 2 Effect of Power Generation Control on Engine Speed

Load	Conventional regulator	LRC regulator
Headlamps (high)	-70rpm	-30rpm
Brakes	-30rpm	-20rpm
Fan	-90rpm	-40rpm
Rear-window defogger	-50rpm	-30rpm

Note: For a 4 cylinder 1.6l engine with ISC (idling setting Ne-800rpm).

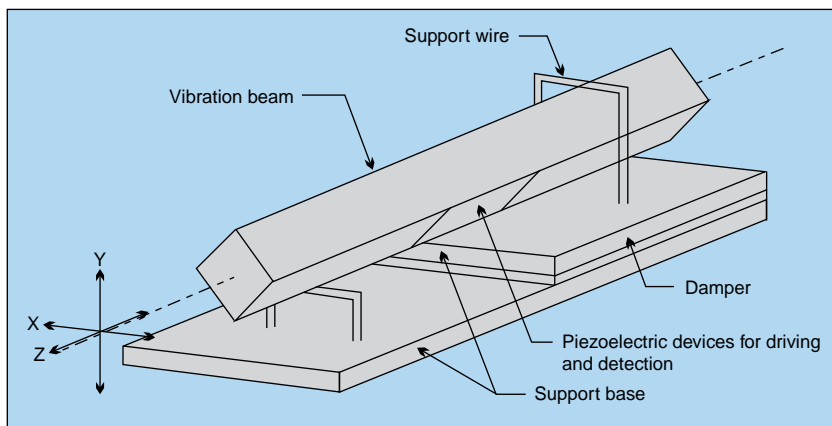
be reduced by about 50rpm, which converts to a 1.4% increase in fuel economy measured by the 10.15 method.

Care in the design of even “minor” engine components such as the starter and alternator can bring substantial benefits to fuel economy. The improvements presented here are likely to be seen in vehicles manufactured in the near future. □

An Angular Velocity Sensor

Angular velocity sensors will form a vital part of future sophisticated vehicle stability control systems. Given the required accuracy and speed of response, they enable a comparison between the actual angular velocity of a vehicle and the angular velocity that would be inferred from the road speed and the angle of the steering wheel. This provides, for instance, an indication of when the vehicle may be skidding.

Mitsubishi Electric has developed a high-resolution sensor based on a vibration beam with two supports that is compact, lightweight and inexpensive. If constant vibration is



Construction of sensor element.

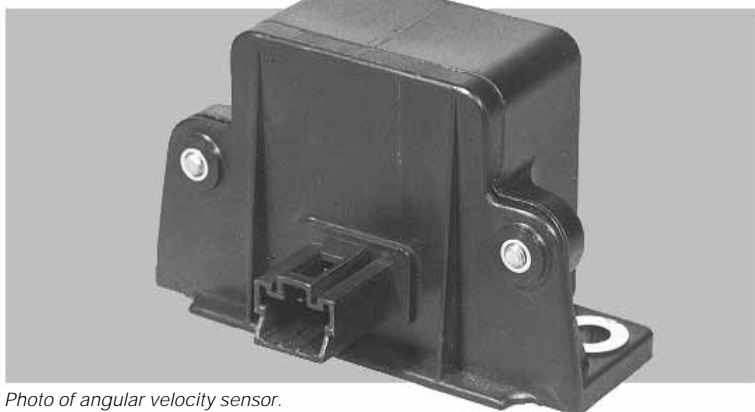
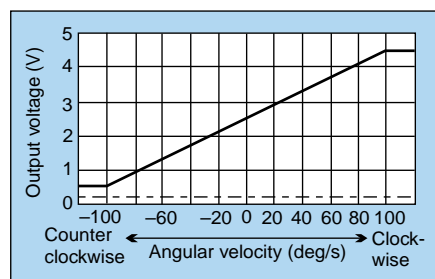


Photo of angular velocity sensor.



key
 — Operational device
 -- Failed device

Output characteristics.

applied in a particular direction, the Coriolis force causes a displacement perpendicular to the direction of the vibration with a magnitude proportional to the angular velocity around the vibration beam. A ceramic piezoelectric vibrator is used to apply vibration to the beam and to measure beam displacement. The sensor also includes circuitry that converts the detector output to an angular velocity signal usable for vehicle stability control. □

Table 1 Specifications

Operating voltage range	8 ~ 16V
Storage temp. range	-40 ~ 85°C
Operating temp. range	-30 ~ 75°C
Angular velocity detection range	-100 ~ 100 deg/s
Static output voltage	2.5V typ. (at 25°C)
DC temperature drift	10 deg/s max.
Sensitivity (scale factor)	20 ±1mV/(deg/s) over operating temperature range
Resolution	0.2 deg/s max.
Linearity (at 25°C)	0.5% of full-scale deflection
External dimensions	85 x 36 x 52mm (including mount)
Weight	100g

Radio with CD Player for the European Market



The radio/CD player for the European market.

Model DH-6581 is a top-end radio with an integrated CD player and radio data system (RDS) functions developed as dealer-installed optional equipment for Mitsubishi Motors vehicles sold in Europe.

In addition to previous RDS functions, Model DH-6581 supports program type (PTY) and enhancement of other network (EON) signals. PTY enables the user to select stations by genre. EON supports automatic program and station selection and functions that enable the unit to serve as a traffic information receiver.

The automatic station search has been enhanced by incorporating two tuning circuits, one that scans rapidly, one slowly. Continuous received-signal noise-level measurements are

fed to a microcomputer that dynamically adjusts reproduction frequency characteristics for optimal reception.

The CD player features a newly developed automatic servo adjustment mechanism that absorbs variations in optical characteristics from disk to disk, ensuring stable playback. A one-bit DAC with an eight-bit oversampling digital filter guarantees high-quality CD sound, and repeat, random and other user playback functions are provided.

The unit features a front panel with curved lines and enlarged LCD for improved legibility, and theft-preventive design. The operating panel can be removed, and the unit has a flashing LED radio/CD player vehicle alarm system indicator. □

An Ionic Current Detection System



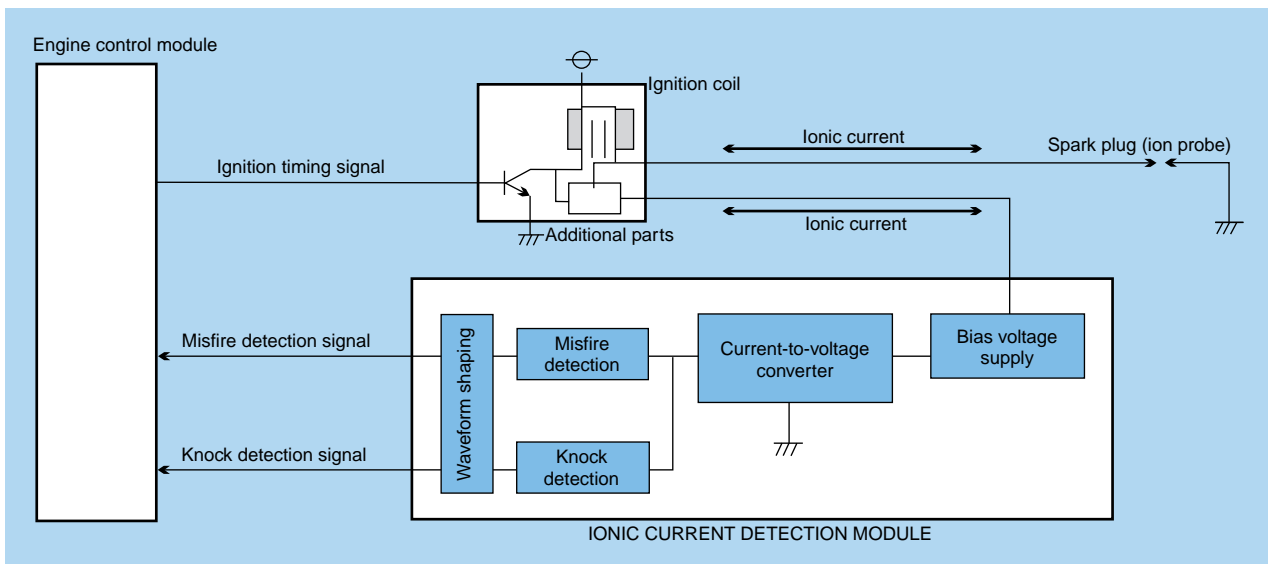
The ionic current detection module.

Mitsubishi Electric has developed a revolutionary sensor that accurately detects engine misfires and the level

of knocking, opening the door to optimized per-cylinder engine control capabilities.

The system can monitor conditions in the cylinders of an internal combustion engine by measuring the currents associated with the ionization that occurs along the flame front during the power stroke. The system employs conventional spark plugs as the ion probes and is easily adapted to any ignition system. It consists of an ignition coil with supplemental electronics, a modified distributor cap (if distributor ignition is used) and an ionic current detection module.

The system contributes to optimized engine control by monitoring each combustion cycle in each cylinder and providing feedback to the engine control system. It requires neither engine structure modifications nor an external high-voltage bias supply. The detector outputs can be easily integrated into the engine control computer. □



Block diagram

Radio with Minidisc Player for the Japanese Market



The radio/Minidisc player for the Japanese market

This product, developed for the '97 model year, combines an AM/FM tuner, Minidisc player and high-power, four-channel amplifier into a compact unit occupying just one DIN mounting slot. This unit and its companion CD player, also newly developed, serve as the flagship products of Mitsubishi Electric's new line of car-audio equipment.

The Minidisc player features a new

silent, quick-response mechanism, a long-stroke damper and a high-capacity memory buffer that enhance shock immunity during playback. User playback functions include cueing, repeat and random play. A one-bit DAC with an eight-bit oversampling digital filter guarantees high-quality Minidisc sound.

The tuner memory stores up to 12 FM stations and six AM stations, and

has an autostore function that automatically registers strong stations. A memory scan function rotates through the preset stations in succession.

The audio unit features a high-power four-channel amplifier, electronic volume control, and RCA-type preamp output jacks. Use of special-purpose audio capacitors maintains the studio quality of digital music sources. Through Mitsubishi Electric's proprietary Diabus, the unit's LCD screen and controls can be used to operate other Diabus equipment including a CD changer, CD player, Minidisc changer and TV tuner.

The modern front housing incorporates a dot-matrix LCD panel that displays Minidisc title information in English or Japanese *kana*. □

MITSUBISHI ELECTRIC OVERSEAS NETWORK (Abridged)

Country	Address	Telephone	
U.S.A.	Mitsubishi Electric America, Inc.	5665 Plaza Drive, P.O. Box 6007, Cypress, California 90630-0007	714-220-2500
	Mitsubishi Electronics America, Inc.	5665 Plaza Drive, P.O. Box 6007, Cypress, California 90630-0007	714-220-2500
	Mitsubishi Consumer Electronics America, Inc.	2001 E. Carnegie Avenue, Santa Ana, California 92705	714-261-3200
	Mitsubishi Semiconductor America, Inc.	Three Diamond Lane, Durham, North Carolina 27704	919-479-3333
	Horizon Research, Inc.	1432 Main Street, Waltham, Massachusetts 02154	617-466-8300
	Mitsubishi Electric Power Products Inc.	Thorn Hill Industrial Park, 512 Keystone Drive, Warrendale, Pennsylvania 15086	412-772-2555
	Mitsubishi Electric Manufacturing Cincinnati, Inc.	4773 Bethany Road, Mason, Ohio 45040	513-398-2220
	Astronet Corporation	37 Skyline Drive, Suite 4100, Lake Mary, Florida 32746-6214	407-333-4900
Canada	Powerex, Inc.	Hills Street, Youngwood, Pennsylvania 15697	412-925-7272
	Mitsubishi Electric Research Laboratories, Inc.	201 Broadway, Cambridge, Massachusetts 02139	617-621-7500
Mexico	Mitsubishi Electric Sales Canada Inc.	4299 14th Avenue, Markham, Ontario L3R 0J2	905-475-7728
	Mitsubishi Electronics Industries Canada Inc.	1000 Wye Valley Road, Midland, Ontario L4R 4L8	705-526-7871
Brazil	Melco de Mexico S.A. de C.V.	Mariano Escobedo No. 69, Tlalnepantla, Edo. de Mexico	5-565-6269
	MELCO do Brazil, Com. e Rep. Ltda.	Av. Rio Branco, 123, a 1507, 20040, Rio de Janeiro	21-221-8343
Argentina	MELCO-TEC Rep. Com. e Assessoria Tecnica Ltda.	Av. Rio Branco, 123, a 1507, 20040, Rio de Janeiro	21-221-8343
	MELCO Argentina S.R.L.	Florida 890-20º-Piso, C.P. 1005, Buenos Aires	1-312-6982
Colombia	MELCO de Colombia Ltda.	Calle 35 No. 7-25, Oficinas No. 1201/02, Edificio, Caxdac, Apartado Aereo 29653, Bogotá	1-287-9277
U.K.	Mitsubishi Electric U.K. Ltd.	Travellers Lane, Hatfield, Herts. AL10 8XB, England	1707-276100
	Apricot Computers Ltd.	3500 Parkside, Birmingham Business Park, Birmingham, B37 7YS, England	21-717-7171
	Mitsubishi Electric Europe Coordination Center	Centre Point (18th Floor), 103 New Oxford Street, London, WC1A 1EB	71-379-7160
France	Mitsubishi Electric France S.A.	55, Avenue de Colmar, 92563, Rueil Malmaison Cedex	1-47-08-78-00
Netherlands	Mitsubishi Electric Netherlands B.V.	3rd Floor, Parnassustoren, Locatellikade 1, 1076 AZ, Amsterdam	20-6790094
Germany	Mitsubishi Electric Europe GmbH	Gothaer Strasse 8, 40880 Ratingen	2102-4860
	Mitsubishi Semiconductor Europe GmbH	Konrad Zuse Strasse 1, 52477 Alsdorf	2404-990
Spain	MELCO Iberica S.A. Barcelona Office	Poligono Industrial "Can Magi", Calle Joan Buscallà 2-4, Apartado de Correos 420, 08190 Sant Cugat del Vallés, Barcelona	3-589-3900
Italy	Mitsubishi Electric Europe GmbH, Milano Office	Centro Direzionale Colleoni, Palazzo Perseo-Ingresso 2, Via Paracelso 12, 20041 Agrate Brianza, Milano	39-60531
China	Shanghai Mitsubishi Elevator Co., Ltd.	811 Jiang Chuan Rd., Minhang, Shanghai	21-4303030
Hong Kong	Mitsubishi Electric (H.K.) Ltd.	41st Floor, Manulife Tower, 169 Electric Road, North Point	510-0555
	Ryoden Holdings Ltd.	10th Floor, Manulife Tower, 169 Electric Road, North Point	887-8870
	Ryoden Merchandising Co., Ltd.	32nd Floor, Manulife Tower, 169 Electric Road, North Point	510-0777
Korea	KEFICO Corporation	410, Dangjung-Dong, Kunpo, Kyunggi-Do	343-51-1403
Taiwan	MELCO Taiwan Co., Ltd.	2nd Floor, Chung-Ling Bldg., No. 363, Sec. 2, Fu-Hsing S. Road, Taipei	2-733-2383
	Shihlin Electric & Engineering Corp.	No. 75, Sec. 6, Chung Shan N. Rd., Taipei	2-834-2662
	China Ryoden Co., Ltd.	Chung-Ling Bldg., No. 363, Sec. 2, Fu-Hsing S. Road, Taipei	2-733-3424
Singapore	Mitsubishi Electric Singapore Pte. Ltd.	152 Beach Road #11-06/08, Gateway East, Singapore 189721	295-5055
	Mitsubishi Electric Sales Singapore Pte. Ltd.	307 Alexandra Road #05-01/02, Mitsubishi Electric Building, Singapore 159943	473-2308
	Mitsubishi Electronics Manufacturing Singapore Pte. Ltd.	3000, Marsiling Road, Singapore 739108	269-9711
	Mitsubishi Electric Asia Coordination Center	307 Alexandra Road #02-02, Mitsubishi Electric Building, Singapore 159943	479-9100
Malaysia	Mitsubishi Electric (Malaysia) Sdn. Bhd.	Plo 32, Kawasan Perindustrian Senai, 81400 Senai, Johor	7-5996060
	Antah MELCO Sales & Services Sdn. Bhd.	3 Jalan 13/1, 46860 Petaling Jaya, Selangor, P.O. Box 1036	3-756-8322
	Ryoden (Malaysia) Sdn. Bhd.	2nd Fl., Wisma Yan, Nos. 17 & 19, Jalan Selangor, 46050 Petaling Jaya	3-755-3277
Thailand	Kang Yong Watana Co., Ltd.	15th Floor, Vanit Bldg., 1126/1, New Petchburi Road, Phayathai, Bangkok 10400	2-255-8550
	Kang Yong Electric Co., Ltd.	67 Moo 11, Bangna-Trad Highway, Km. 20 Bang Plee, Samutprakarn 10540	2-312-8151
	MELCO Manufacturing (Thailand) Co., Ltd.	86 Moo 4, Km. 23 Bangna-Trad, Bangplee, Semudparkarn 10540	2-312-8350-3
	Mitsubishi Elevator Asia Co., Ltd.	Bangpakong Industrial Estate, 700/86-92, Moo 6 Tambon Don Hua Roh, Muang District Chonburi 20000	38-213-170
Philippines	Mitsubishi Electric Asia Coordination Center (Thailand)	17th Floor, Bangna Tower, 2/3 Moo 14, Bangna-Trad Highway 6.5 Km, Bangkawe, Bang Plee, Samutprakarn 10540	2-312-0155-7
	International Elevator & Equipment, Inc.	Km. 23 West Service Road, South Superhighway, Cupang, Muntinlupa, Metro Manila	2-842-3161-5
Australia	Mitsubishi Electric Australia Pty. Ltd.	348 Victoria Road, Postal Bag No. 2, Rydalmere, N.S.W. 2116	2-684-7200
New Zealand	MELCO Sales (N.Z.) Ltd.	1 Parliament St., Lower Hutt, P.O. Box 30-772 Wellington	4-569-7350
Representatives			
China	Mitsubishi Electric Corp. Beijing Office	SCITE Tower, Rm. 1609, Jianguo Menwai, Dajie 22, Beijing	1-512-3222
	Mitsubishi Electric Corp. Shanghai Office	Room No. 1506-8, Shanghai Union Building 100, Yanan-East Street, Shanghai	21-320-2010
Korea	Mitsubishi Electric Corp. Seoul Office	Daehan Kyoyuk Insurance Bldg., Room No. 1204 #1, Chongno 1-ka, Chongno-ku, Seoul	2-732-1531-2
Viet Nam	Mitsubishi Electric Corp. Ho Chi Minh City Office	8 B2, Han Nam Officetel 65, Nguyen Du St., 1st District, Ho Chi Minh City	8-243-984

